Fatigue Life Prediction using 2-Scale Temporal Asymptotic Homogenization

Caglar Oskay and Jacob Fish
Civil and Environmental Engineering Department
Rensselaer Polytechnic Institute, Troy, NY, 12180, USA

Abstract

In this manuscript, fatigue of structures is modeled as a multiscale phenomenon in time domain. Multiple temporal scales are introduced due to the fact that the load period is orders of magnitude smaller than the useful life span of a structural component. The problem of fatigue life prediction is studied within the framework of mathematical homogenization with two temporal coordinates. By this approach the original initial boundary value problem is decomposed into coupled micro-chronological (fast time-scale) and macro-chronological (slow time-scale) problems. The life prediction methodology has been implemented in ABAQUS and validated against direct cycle-by-cycle simulations.

Keywords: fatigue life prediction, crack propagation, temporal homogenization, brittle damage, cohesive model

1 Introduction

Fatigue of structures is a multiscale phenomenon in space and time. It is multiscale in space because a crack (or microcrack) size may be of several orders of magnitude smaller than a structural component of interest. It is multiscale in time because the load period could be in the order of seconds whereas the component life may span years. Given this tremendous disparity of spatial and temporal scales, life predictions pose a great challenge to mechanics and materials science communities.

Fatigue life prediction methods range from experimentation, to modeling and computational resolution of spatial scales. The basic design tool today is primarily experimental, based on so called S-N curves, which provide the component life versus cyclic stress level. Since there is a scatter of fatigue life data, a family of S-N curves with probability of failure known as S-N-P plots are often used. Fatigue experiments are generally limited to specimens or small structural components, and therefore, boundary and initial conditions between the component or interconnect of interest and the remaining structure involves some sort of modeling. Typically finite element analysis is carried out to predict the ”far fields” acting on the critical component or interconnect. These types of calculations do not take into account force redistribution caused by accumulation of damage taking place in the critical components or interconnects.

Paris law [1] represents one of the first attempts to empirically model fatigue life. It states that under ideal conditions of high cycle fatigue (or small scale yielding) and constant amplitude loading, the growth rate of long cracks depends on the amplitude of the stress intensity factors.

Models departing from these ideal conditions have also been documented (e.g., [2, 3, 4, 5, 6]). Various crack growth ”laws” are being used in conjunction with multiple spatial scales methods which allow for propagation of arbitrary discontinuities in a fixed mesh (e.g., [7, 8]).

An attempt to resolve the temporal scales, i.e., to carry out cycle-by-cycle simulation, in conjunction with a cohesive law crack model based on unloading-reloading hysteresis has been recently reported by Nguyen et al. [9]. Cycle-by-cycle simulation, however, may not be feasible for large scale systems undergoing high cycle fatigue. Nevertheless, an attractive feature of this approach is that it allows for a unified treatment of long and short cracks and the effects of overloads.

The first multiscale computational technique in the time domain, known as the ”cycle jump” technique [10, 11], has been proposed in the context of continuum damage mechanics. By this approach a single load cycle is used to compute the rate of fatigue damage growth at each spatial integration point and then to construct an ordinary differential equation [12]:

$$\frac{d\omega(x_a)}{dN} = \omega_K(x_a) - \omega_{K-1}(x_a) \tag{1}$$

where $\omega(x_a)$ is the damage variable at the integration point a; N is the cycle variable; K is the cycle count; and, ω_K and ω_{K-1} are the states of the damage variable at the end of K^{th} and $(K-1)^{\text{th}}$ cycles, respectively. Adaptive integrators have been used to control the accuracy of the integration [12]. Unfortunately, while advancing the state variables (damage variables) the constitutive equations are violated requiring adjustment of governing equations, which may not be unique.

In this paper we present a new paradigm for multiscale modeling of fatigue based on multiple temporal scale asymptotic analysis. The proposed methodology hinges on the hypothesis of local periodicity in the time domain - the concept that serves the foundation of the spatial homogenization theory [13]. In the temporal homogenization proposed here, both the applied loads and the response fields are assumed to depend on a slow time coordinate, t (slow degradation of material properties due to fatigue), as well as on the fast time coordinate, τ (due to locally periodic loading). The concept of local periodicity implies that at the neighboring points in the time domain (same t), homologous by periodicity (same τ), the value of the function is the same, but at points homologous by periodicity but separated in t, the value of the function can be different. In case of overloads, temporal scales cannot be separated, and thus, the solution has to be resolved in the portion of the time domain where the overloads are present, while elsewhere in the time domain the temporal homogenization theory developed here can be exercised.

The theory is developed for the case of accumulation of distributed damage (microvoids or microcracks) and propagation of macrocracks up to failure. For the latter, a cohesive crack model in the form of continuum damage mechanics exhibiting unloading-reloading hysteresis developed by Fish and Yu [12] is adopted. Classical crack growth models cannot be applied to direct cycle-by-cycle simulation due to the nondissipative nature of these models for subcritical cyclic loading. Crack closure is enforced by selecting appropriate parameters within the damage model that effectively serve as a penalty function. In the case of distributed damage, continuum damage mechanics exhibiting unloading-reloading hysteresis [12] is employed. Damage evolution in the form of a power law along the lines of viscoplasticity is used as a regularization of local softening behavior.

2 Problem statement for solids undergoing fatigue damage

In the present study, multiple temporal scales are introduced to model slow degradation of material properties due to fatigue, as well as to resolve the deformation within a single load cycle. The *macro-chronological* scale is denoted by the intrinsic time coordinate, t, while the *micro-chronological* scale is denoted by the fast time coordinate, τ. A local periodicity (τ-periodicity) assumption is made for field variables (unless otherwise stated), similar to Y-periodicity in spatial homogenization theory. The two scales defined above are related by a small positive scaling parameter, ζ:

$$\tau = \frac{t}{\zeta}; \quad \zeta \ll 1 \tag{2}$$

The periodic response fields, ϕ, are defined to accommodate the presence of multiple temporal scales:

$$\phi^\zeta(\mathbf{x},t) = \phi(\mathbf{x},t,\tau(t)) \tag{3}$$

where $\mathbf{x}$ represents the spatial coordinates. Time differentiation in the presence of multiple temporal scales is given by the chain rule:

$$\dot{\phi}^\zeta(\mathbf{x},t) = \phi_{,t}(\mathbf{x},t,\tau) + \frac{1}{\zeta}\phi_{,\tau}(\mathbf{x},t,\tau) \tag{4}$$

in which a comma followed by a subscript coordinate denotes partial derivative, and superposed dot denotes the total time derivative.

2.1 Failure by accumulation of distributed damage

The failure mechanism of some brittle materials, such as ceramics and concrete, is characterized by only minor plastic flow, and is dominated by degradation of material properties due to nucleation, growth and coalescence of microcracks [14, 15]. Furthermore, the resulting propagation of large cracks usually takes place at a significantly higher rate and constitutes a small portion of the fatigue life. Continuous damage mechanics (CDM) provide a theoretical framework to model this type of failure [16]. In CDM, a continuous tensorial quantity, $\mathbf{M}$, is defined to represent the state of damage, and introduced into the constitutive laws using the thermodynamics of irreversible processes. The order of $\mathbf{M}$ generally depends on the properties of the material as well as the structure and geometry of the microdefects [14]. In the case of isotropy, the state of damage may be represented by a scalar variable, $\omega^\zeta = \omega(\mathbf{x},t,\tau) \in [0,1)$, such that $\mathbf{M} = (1-\omega^\zeta)\mathbf{I}$, in which $\mathbf{I}$ is the fourth order identity tensor. Damage process may be introduced by considering the free energy density, ψ^ζ, of the form [17]:

$$\psi^\zeta(\omega^\zeta,\boldsymbol{\varepsilon}^\zeta) = (1-\omega^\zeta)\psi_e^\zeta(\boldsymbol{\varepsilon}^\zeta) \tag{5}$$

where ψ_e^ζ is elastic free energy density. For small elastic deformations:

$$\psi_e^\zeta = \frac{1}{2}\boldsymbol{\varepsilon}^\zeta : \mathbf{L} : \boldsymbol{\varepsilon}^\zeta \tag{6}$$

where, $\boldsymbol{\varepsilon}^\zeta$ is the strain tensor, and $\mathbf{L}$ is the fourth order elastic isotropic constitutive tensor. For an isothermal process (i.e., constant temperature), the Clausius-Duhem inequality takes the form; $\dot{\psi}^\zeta \geq \boldsymbol{\sigma}^\zeta : \dot{\boldsymbol{\varepsilon}}^\zeta$. Differentiating (5) and using the Clausius-Duhem inequality, the following constitutive equation and the condition of irreversible damage is obtained:

$$\boldsymbol{\sigma}^\zeta = \frac{\partial\psi^\zeta(\omega^\zeta,\boldsymbol{\varepsilon}^\zeta)}{\partial\boldsymbol{\varepsilon}^\zeta} = (1-\omega^\zeta)\mathbf{L} : \boldsymbol{\varepsilon}^\zeta; \quad \dot{\omega}^\zeta\psi_e^\zeta \geq 0 \tag{7}$$

in which $\boldsymbol{\sigma}^\zeta$ is the stress tensor.

The initial boundary value problem (IBVP) for a continuous damage process may then be expressed as:

$$\begin{aligned}
&\text{Equilibrium equation:} & \nabla\cdot\boldsymbol{\sigma}^{\zeta} &+ \mathbf{b}(\mathbf{x},t,\tau)=\mathbf{0} & &\text{on } \Omega\times(0,t_o)\times(0,\tau_o) && \text{(8a)}\\
&\text{Constitutive equation:} & \boldsymbol{\sigma}^{\zeta} &= (1-\omega^{\zeta})\,\mathbf{L}:\boldsymbol{\varepsilon}^{\zeta} & &\text{on } \Omega\times(0,t_o)\times(0,\tau_o) && \text{(8b)}\\
&\text{Kinematic equation:} & \boldsymbol{\varepsilon}^{\zeta} &= \frac{1}{2}(\nabla\mathbf{u}^{\zeta}+\mathbf{u}^{\zeta}\nabla) & &\text{on } \Omega\times(0,t_o)\times(0,\tau_o) && \text{(8c)}\\
&\text{Initial condition:} & \mathbf{u}^{\zeta} &= \tilde{\mathbf{u}}(\mathbf{x}) & &\text{on } \Omega && \text{(8d)}\\
&\text{Boundary conditions:} & \mathbf{u}^{\zeta} &= \bar{\mathbf{u}}(\mathbf{x},t,\tau) & &\text{on } \Gamma_u\times(0,t_o)\times(0,\tau_o) && \text{(8e)}\\
& & \boldsymbol{\sigma}^{\zeta}\mathbf{n} &= \mathbf{f}(\mathbf{x},t,\tau) & &\text{on } \Gamma_f\times(0,t_o)\times(0,\tau_o) && \text{(8f)}
\end{aligned}$$

in which ∇ is the vector differential operator given by $\nabla=(\partial/\partial x_1,\ \partial/\partial x_2,\ \partial/\partial x_3)$ in Cartesian coordinate system; $\mathbf{b}$ is the body force; $\mathbf{u}^{\zeta}$ is the displacement vector; t_o is the observation time in macro-chronological (slow) time coordinate; τ_o is the load period in micro-chronological (fast) time coordinate; Ω and Γ are the spatial problem domain and its boundary, respectively; $\tilde{\mathbf{u}}$ is the initial displacement field; $\bar{\mathbf{u}}$ and $\mathbf{f}$ are prescribed displacements and tractions on the boundaries Γ_u and Γ_f, respectively, where $\Gamma=\Gamma_u\cup\Gamma_f$ and $\Gamma_u\cap\Gamma_f$=0.

When monotonic loading is considered, the evolution of the isotropic continuum damage variable, ω^{ζ}, is chosen to be a function of a history variable, κ, which is characterized by the Kuhn-Tucker conditions:

$$\dot{\kappa}\geq 0,\quad \upsilon^{\zeta}-\kappa\leq 0,\quad \dot{\kappa}(\upsilon^{\zeta}-\kappa)=0 \tag{9}$$

in which damage equivalent strain, υ^{ζ}, is generally taken to be some measure of strains. Equation (9) represents the sufficient conditions of the irreversible damage accumulation. For locally periodic loading, unloading-reloading cycles at subcritical load levels also contribute to the accumulation of damage and must be reflected in the description of damage variable, ω^{ζ}. Such a model, previously developed by Fish and Yu [12] was adopted in this study.

The viscoplasticity like damage evolution model [12] represents the accumulation of fatigue damage due to cyclic loading:

$$\dot{\omega}^{\zeta}(\mathbf{x},t)=\begin{cases} 0 & \upsilon^{\zeta}<\upsilon_{ini}\\ \left(\dfrac{\theta^{\zeta}}{\omega^{\zeta}}\right)^{\gamma}\dfrac{\partial\theta^{\zeta}}{\partial\upsilon^{\zeta}}\langle\dot{\upsilon}^{\zeta}\rangle_{+} & \upsilon^{\zeta}\geq\upsilon_{ini}\end{cases} \tag{10}$$

where $\langle\cdot\rangle_{+}=[(\cdot)+|\cdot|]/2$ are MacCauley brackets; $|\cdot|$ denote the absolute value operator; υ_{ini} is a threshold value of υ^{ζ} which represents a domain in strain space where no damage can be accumulated regardless of the loading path; γ is a material parameter representing sensitivity to cyclic loading, and θ^{ζ} is a function of damage equivalent strain, which determines the evolution of damage. In this study, a smooth damage evolution model [12] was adopted:

$$\theta^{\zeta}(\mathbf{x},t)=\frac{\arctan\left[\alpha\left(\dfrac{\langle\upsilon^{\zeta}-\upsilon_{ini}\rangle_{+}}{\upsilon_o}\right)-\beta\right]+\arctan\beta}{\dfrac{\pi}{2}+\arctan\beta} \tag{11}$$

where α, β and υ_o are material constants, and υ^{ζ} is the damage equivalent strain defined as the square root of the energy release rate [17]:

$$\upsilon^{\zeta}=\sqrt{\frac{1}{2}\boldsymbol{\varepsilon}^{\zeta}:\mathbf{L}:\boldsymbol{\varepsilon}^{\zeta}} \tag{12}$$

Tensile loading generally leads to a higher rate of damage accumulation when compared to compression loading [18]. This effect may be modeled by introducing a weighting tensor, $\mathbf{F}^{\zeta}$, and by altering (12) such that:

$$\upsilon^{\zeta} = \sqrt{\frac{1}{2}\left(\mathbf{F}^{\zeta}\hat{\boldsymbol{\varepsilon}}^{\zeta}\right)\hat{\mathbf{L}}\left(\mathbf{F}^{\zeta}\hat{\boldsymbol{\varepsilon}}^{\zeta}\right)} \tag{13}$$

where $\hat{\boldsymbol{\varepsilon}}^{\zeta}$ is the principal strain vector; $\hat{\mathbf{L}} \equiv \hat{L}_{\varsigma\eta} = L_{\varsigma\varsigma\eta\eta}$ is the elastic isotropic constitutive tensor projected onto the principal directions ($\varsigma, \eta = 1, 2, 3$ and no summation is implied for Greek indices). The strain weighting matrix, $\mathbf{F}^{\zeta}$, is defined as:

$$\mathbf{F}^{\zeta} = \begin{bmatrix} h_1^{\zeta} & 0 & 0 \\ 0 & h_2^{\zeta} & 0 \\ 0 & 0 & h_3^{\zeta} \end{bmatrix} \tag{14}$$

$$\mathbf{h}^{\zeta}(\hat{\boldsymbol{\varepsilon}}^{\zeta}) = \frac{1}{2} + \frac{1}{\pi}\arctan\left[a_1(\hat{\boldsymbol{\varepsilon}}^{\zeta} - a_2)\right] \tag{15}$$

in which $\mathbf{h}^{\zeta}$ is a vector composed of the diagonal components of $\mathbf{F}^{\zeta}$, and a_1 and a_2 are material parameters.

A bifurcation analysis was conducted to study the localization characteristics of the fatigue damage cumulative law under subcritical periodic loading conditions. The analysis, described in Appendix B, shows that the proposed model acts as a localization limiter when the material parameter, γ, is taken to be a function of the strain tensor and the loading history.

2.2 Failure by crack propagation

The response of quasi-brittle and ductile materials is generally dominated by the propagation of a distinct macrocrack [19]. Cohesive theories of fracture have been applied to describe such processes under monotonic (e.g., [20]) as well as cyclic (e.g., [9]) loading. In this paper such a cohesive law was used to model the propagation of macrocracks under fatigue loads. The direction of propagation is predefined and only small-scale yielding is considered. Under these conditions, the IBVP may be posed by replacing the constitutive equation, (8b), by a linear elastic law ($\boldsymbol{\sigma}^{\zeta} = \mathbf{L} : \boldsymbol{\varepsilon}^{\zeta}$) and considering a predefined cohesive zone; Γ_c.

Following Ortiz and Pandolfi [21] a free energy density in the cohesive zone takes a general form (for an isothermal process):

$$\psi_c^{\zeta} = \psi_c^{\zeta}(\mathbf{d}^{\zeta}, \omega^{\zeta}) \tag{16}$$

where $\mathbf{d}^{\zeta}$ is the crack opening displacement at the cohesive zone. We assume a linear dependence between ω^{ζ} and ψ_c^{ζ}:

$$\psi_c^{\zeta} = \frac{1}{2}(1 - \omega^{\zeta})\, k (d^{\zeta})^2 \tag{17}$$

$$d^{\zeta} = \|\mathbf{d}^{\zeta}\| \tag{18}$$

in which k is the initial loading stiffness, and $\|\cdot\|$ is the Euclidean norm. Using the Clausius-Duhem inequality and arguments presented in the previous section, it can be shown that:

$$\mathbf{t}^{\zeta} = \frac{\partial \psi_c^{\zeta}}{\partial \mathbf{d}^{\zeta}} \tag{19}$$

where $\mathbf{t}^{\zeta}$ is the traction along Γ_c. Inserting (17) into (19) we obtain the constitutive equation at the cohesive zone:

$$\mathbf{t}^{\zeta} = \frac{1}{d^{\zeta}} \frac{\partial \psi_c^{\zeta}}{\partial d^{\zeta}} \mathbf{d}^{\zeta} \tag{20}$$

The evolution of damage is modeled using a fatigue cumulative damage law, similar to that presented in the previous section. In this case, the damage equivalent strain is expressed in terms of the crack opening displacement:

$$\upsilon_c^{\zeta} = \sqrt{\frac{1}{2}k\left(hd_n^{\zeta} + wd_s^{\zeta}\right)^2} \tag{21}$$

where $d_n^{\zeta} = \mathbf{d}^{\zeta}\mathbf{n}$; $d_s^{\zeta} = \mathbf{d}^{\zeta} - d_n^{\zeta}\mathbf{n}$; $\mathbf{n}$ is the unit normal to Γ_c; $h(d_n^{\zeta})$ and $w(d_s^{\zeta})$ are the weighting functions (similar to (15)) of crack opening and sliding modes, respectively.

3 Two-scale temporal asymptotic analysis of solids subjected to periodic loading

We start by representing the displacement field, $\mathbf{u}^{\zeta}$, using a two-scale asymptotic expansion:

$$\mathbf{u}^{\zeta} = \sum_{m=0,1,\ldots} \zeta^m \mathbf{u}^m(\mathbf{x},t,\tau) \tag{22}$$

where $\mathbf{u}^m$ are periodic functions. Using (22) and the chain rule, strain and strain rate fields may be expressed as:

$$\boldsymbol{\varepsilon}^{\zeta} = \sum_{m=0,1,\ldots} \zeta^m \boldsymbol{\varepsilon}^m(\mathbf{x},t,\tau); \qquad \boldsymbol{\varepsilon}^m = \frac{1}{2}\left(\nabla\mathbf{u}^m + \mathbf{u}^m\nabla\right) \tag{23}$$

$$\dot{\boldsymbol{\varepsilon}}^{\zeta} = \sum_{m=0,1,\ldots} \zeta^{m-1} \dot{\boldsymbol{\varepsilon}}^{m-1}(\mathbf{x},t,\tau); \qquad \dot{\boldsymbol{\varepsilon}}^{-1} = \boldsymbol{\varepsilon}^{0}_{,\tau}, \quad \text{and} \quad \dot{\boldsymbol{\varepsilon}}^{m} = \boldsymbol{\varepsilon}^{m}_{,t} + \boldsymbol{\varepsilon}^{m+1}_{,\tau} \tag{24}$$

The fatigue damage variable, ω^{ζ}, and the stress field, $\boldsymbol{\sigma}^{\zeta}$, are also approximated using expansions in the form of (22):

$$\omega^{\zeta} = \sum_{m=0,1,\ldots} \zeta^m \omega^m(\mathbf{x},t,\tau), \qquad \boldsymbol{\sigma}^{\zeta} = \sum_{m=0,1,\ldots} \zeta^m \boldsymbol{\sigma}^m(\mathbf{x},t,\tau) \tag{25}$$

Considering failure by accumulation of distributed damage and inserting the asymptotic representations of the strain and stress fields, and damage variable into (8b), various orders of the constitutive equation are obtained ($m = 0, 1, \ldots$):

$$O(\zeta^0): \qquad \boldsymbol{\sigma}^0 = (1-\omega^0)\mathbf{L}:\boldsymbol{\varepsilon}^0 \tag{26}$$

$$O\left(\zeta^{m+1}\right): \qquad \boldsymbol{\sigma}^{m+1} = (1-\omega^0)\mathbf{L}:\boldsymbol{\varepsilon}^{m+1} - \sum_{s=1}^{m+1}\omega^s\mathbf{L}:\boldsymbol{\varepsilon}^{m+1-s} \tag{27}$$

Alternatively, the constitutive equations may be represented in the rate form by using (24) and the time derivatives of (26-27). The leading order constitutive equation becomes:

$$O\left(\zeta^{-1}\right): \qquad \boldsymbol{\sigma}^{0}_{,\tau} = (1-\omega^0)\mathbf{L}:\boldsymbol{\varepsilon}^{0}_{,\tau} - \omega^{0}_{,\tau}\mathbf{L}:\boldsymbol{\varepsilon}^0 \tag{28}$$

and higher order equations may be written in the following form:

$$O(\zeta^m): \qquad \boldsymbol{\sigma}^{m}_{,t} = \mathbf{L}:\boldsymbol{\varepsilon}^{m}_{,t} - \sum_{s=0}^{m}\omega^s\mathbf{L}:\boldsymbol{\varepsilon}^{m-s}_{,t} - \sum_{s=0}^{m}\omega^{s}_{,t}\mathbf{L}:\boldsymbol{\varepsilon}^{m-s} \tag{29a}$$

$$\boldsymbol{\sigma}^{m+1}_{,\tau} = \mathbf{L}:\boldsymbol{\varepsilon}^{m+1}_{,\tau} - \sum_{s=0}^{m+1}\omega^s\mathbf{L}:\boldsymbol{\varepsilon}^{m+1-s}_{,\tau} - \sum_{s=0}^{m+1}\omega^{s}_{,\tau}\mathbf{L}:\boldsymbol{\varepsilon}^{m+1-s} \tag{29b}$$

Various orders of the equilibrium equation are obtained by substituting the expanded stress field into (8a):

$$O(1) \quad : \quad \nabla \cdot \boldsymbol{\sigma}^{o} + \mathbf{b}(\mathbf{x},t,\tau) = \mathbf{0} \qquad \text{on } \Omega \times (0,t_o) \times (0,\tau_o) \tag{30}$$

$$O\left(\zeta^{m+1}\right) \quad : \quad \nabla \cdot \boldsymbol{\sigma}^{m+1} = \mathbf{0} \qquad \text{on } \Omega \times (0,t_o) \times (0,\tau_o) \tag{31}$$

Similarly, the initial and boundary conditions may be described using the expanded representations of displacement and stress fields along with (8d-8f):

$$O(1): \qquad \mathbf{u}^{o}(\mathbf{x}, t=\tau=0) = \tilde{\mathbf{u}}(\mathbf{x}) \qquad \text{on } \Omega \tag{32}$$

$$\mathbf{u}^{o} = \bar{\mathbf{u}}(\mathbf{x},t,\tau) \qquad \text{on } \Gamma_u \times (0,t_o) \times (0,\tau_o) \tag{33}$$

$$\boldsymbol{\sigma}^{o}\mathbf{n} = \mathbf{f}(\mathbf{x},t,\tau) \qquad \text{on } \Gamma_f \times (0,t_o) \times (0,\tau_o) \tag{34}$$

The initial and boundary conditions for higher order problems are trivial.

The equilibrium and constitutive equations, along with the initial and boundary conditions of equal orders are sought to be decomposed into micro- and macro-chronological IBVPs. A temporal smoothing operator is, therefore, introduced [22]:

$$\langle \cdot \rangle = \frac{1}{\tau_o} \int_0^{\tau_o} \cdot \; d\tau \tag{35}$$

The decomposition of the displacement, strain and stress fields are evaluated using the temporal smoothing operator:

$$\mathbf{u}^{m}(\mathbf{x},t,\tau) = \langle \mathbf{u}^{m} \rangle (\mathbf{x},t) + \boldsymbol{\chi}^{m}(\mathbf{x},t,\tau) \tag{36a}$$

$$\boldsymbol{\varepsilon}^{m}(\mathbf{x},t,\tau) = \langle \boldsymbol{\varepsilon}^{m} \rangle (\mathbf{x},t) + \boldsymbol{\Psi}^{m}(\mathbf{x},t,\tau) \tag{36b}$$

$$\boldsymbol{\sigma}^{m}(\mathbf{x},t,\tau) = \langle \boldsymbol{\sigma}^{m} \rangle (\mathbf{x},t) + \boldsymbol{\Phi}^{m}(\mathbf{x},t,\tau) \tag{36c}$$

in which $\langle \cdot \rangle$ denote the macro-chronological fields; $\boldsymbol{\chi}^m$, $\boldsymbol{\Psi}^m$, $\boldsymbol{\Phi}^m$ represent the micro-chronological portion of the displacement, strain and stress fields, respectively. Damage variable, ω^{ζ}, is cumulative and irreversible in nature and, therefore, not τ-periodic ($\langle \omega^{m}_{,\tau} \rangle \neq 0$). Each unload-reload cycle (hence, each *unit cell* in time) increases the value of the damage variable. It is convenient to introduce a somewhat different decomposition to the damage variable:

$$\omega^{m}(\mathbf{x},t,\tau) = \tilde{\omega}^{m}(\mathbf{x},t) + \Lambda^{m}(\mathbf{x},t,\tau) \tag{37}$$

in which $\tilde{\omega}^m$ and Λ^m are macro- and micro-chronological strain induced damage variables, respectively, to be subsequently described.

The micro-chronological portion of the $O(1)$ constitutive equation may then be obtained by applying the strain, stress, and damage variable decompositions, (36b-37) to (28). At a given instant of the slow time coordinate, t:

$$\boldsymbol{\Phi}^{o}_{,\tau} = (1 - \Lambda^{o}) \mathbf{L} : \boldsymbol{\Psi}^{o}_{,\tau} - \Lambda^{o}_{,\tau} \mathbf{L} : \boldsymbol{\Psi}^{o} - \tilde{\omega}^{o} \mathbf{L} : \boldsymbol{\Psi}^{o}_{,\tau} - \Lambda^{o}_{,\tau} \mathbf{L} : \langle \boldsymbol{\varepsilon}^{o} \rangle \quad \text{on } \Omega \times (0,\tau_o) \tag{38}$$

The macro-chronological portion of the $O(1)$ constitutive equation is obtained by applying the averaging operator on (29a) and exploiting the definitions given in (36b-37):

$$\langle \boldsymbol{\sigma}^{o} \rangle_{,t} = (1 - \tilde{\omega}^{o}) \mathbf{L} : \langle \boldsymbol{\varepsilon}^{o} \rangle_{,t} - \tilde{\omega}^{o}_{,t} \mathbf{L} : \langle \boldsymbol{\varepsilon}^{o} \rangle - \langle \Lambda^{o} \mathbf{L} : \boldsymbol{\varepsilon}^{o} \rangle_{,t} \quad \text{on } \Omega \times (0,t_o) \tag{39}$$

The last term in (39) may be evaluated using a Taylor expansion in fast time coordinate ,τ:

$$\langle \Lambda^{o}(\mathbf{x},t,\tau) \mathbf{L} : \boldsymbol{\varepsilon}^{o} \rangle = \Lambda^{o}(\mathbf{x},t,\tau_1) \mathbf{L} : \langle \boldsymbol{\varepsilon}^{o} \rangle + \Lambda^{o}_{,\tau}(\mathbf{x},t,\tau_1) \mathbf{L} : \langle (\tau - \tau_1) \boldsymbol{\varepsilon}^{o} \rangle + \ldots \tag{40}$$

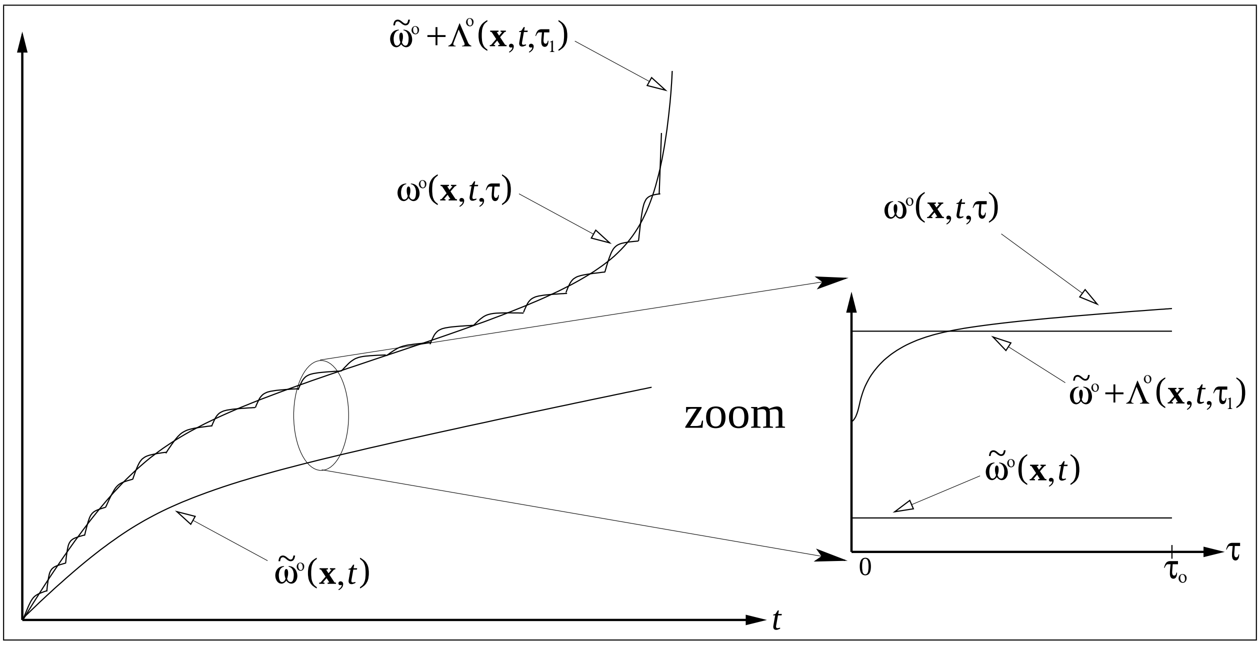

Figure 1: Schematic interpretations of the micro- and macro-chronological strain induced damage variables.

where $\tau_1 \in (0, \tau_o)$. Furthermore for purely tensile or compressive loading; i.e., when:

$$\boldsymbol{\varepsilon}^o\left(\mathbf{x}, t, \tau^+\right) \boldsymbol{\varepsilon}^o\left(\mathbf{x}, t, \tau^-\right) \geq 0 \quad \forall \tau \in (0, \tau_o) \tag{41}$$

where $\tau^{\pm} = \tau \pm \xi$ and $\xi \ll 1$ is a small positive constant. Using mean value theorem, it can be shown that there exists a τ_1 for which $\langle(\tau - \tau_1)\boldsymbol{\varepsilon}^o\rangle = 0$ ($\tau_1 = \tau_o/2$ in case of symmetry). Inserting (40) into (39) and using the above argument:

$$\langle\boldsymbol{\sigma}^o\rangle_{,t} = \left(1 - \tilde{\omega}^o - \Lambda^o(\mathbf{x}, t, \tau_1)\right)\mathbf{L} : \langle\boldsymbol{\varepsilon}^o\rangle_{,t} - \left(\tilde{\omega}^o_{,t} + \Lambda^o_{,t}(\mathbf{x}, t, \tau_1)\right)\mathbf{L} : \langle\boldsymbol{\varepsilon}^o\rangle \tag{42}$$

Figure 1 displays the graphical interpretations of the micro- and macro-chronological strain induced damage variables.

Taking a total time derivative of the asymptotic expansion of the damage variable given in (25) yields:

$$\dot{\omega}^{\zeta} = \sum_{m=0,1,\ldots} \zeta^{m-1}\dot{\omega}^{m-1}(\mathbf{x}, t, \tau); \quad \dot{\omega}^{-1} = \omega^o_{,\tau} \quad \text{and,} \quad \dot{\omega}^m = \omega^m_{,t} + \omega^{m+1}_{,\tau} \tag{43}$$

Similarly,

$$\theta^{\zeta} = \sum_{m=0,1,\ldots} \zeta^m \theta^m(\mathbf{x}, t, \tau), \qquad \upsilon^{\zeta} = \sum_{m=0,1,\ldots} \zeta^m \upsilon^m(\mathbf{x}, t, \tau) \tag{44}$$

$$\dot{\upsilon}^{\zeta} = \sum_{m=0,1,\ldots} \zeta^{m-1}\dot{\upsilon}^{m-1}(\mathbf{x}, t, \tau); \quad \dot{\upsilon}^{-1} = \upsilon^o_{,\tau} \quad \text{and,} \quad \dot{\upsilon}^m = \upsilon^m_{,t} + \upsilon^{m+1}_{,\tau} \tag{45}$$

Using the above approximations, the asymptotic expansion of the damage evolution law presented in (10) can be expressed as (for a damage process; i.e., $\upsilon^o \geq \upsilon_{ini}$, $\upsilon^1 \geq 0$ and $\upsilon^o_{,\tau} > 0$):

$$\begin{aligned}\dot{\omega} = \frac{1}{\zeta}\omega^o_{,\tau} + \omega^o_{,t} + \omega^1_{,\tau} + O(\zeta) = &\left[\left(\frac{\theta^o}{\omega^o}\right)^{\gamma} + \zeta\gamma\left(\frac{\theta^o}{\omega^o}\right)^{\gamma}\left(\frac{\theta^1}{\theta^o} - \frac{\omega^1}{\omega^o}\right) + O(\zeta^2)\right]\cdot \\ &\left[\frac{1}{\zeta}\frac{\partial\theta^o}{\partial\upsilon^o}\upsilon^o_{,\tau} + \frac{\partial\theta^o}{\partial\upsilon^o}\upsilon^o_{,t} + \frac{\partial\theta^1}{\partial\upsilon^o}\upsilon^o_{,\tau} + \frac{\partial\theta^1}{\partial\upsilon^1}\upsilon^1_{,\tau} + O(\zeta)\right]\end{aligned} \tag{46}$$

where the material parameter γ is assumed to be constant. The equation is trivial for unloading and elastic loading (i.e., when $\upsilon^o < \upsilon_{ini}$ or $\upsilon^1 < 0$ or $\upsilon^o_{,\tau} < 0$). The fatigue damage model of order $O(\zeta^{-1})$ may then be approximated by matching lowest order terms in (46):

$$\Lambda^o_{,\tau}(\mathbf{x},t,\tau) = \omega^o_{,\tau}(\mathbf{x},t,\tau) = \begin{cases} 0 & \upsilon^o < \upsilon_{ini} \\ \left(\dfrac{\theta^o}{\omega^o}\right)^\gamma \dfrac{\partial\theta^o}{\partial\upsilon^o}\langle\upsilon^o_{,\tau}\rangle_+ & \upsilon^o \geq \upsilon_{ini} \end{cases} \tag{47}$$

Furthermore, order $O(1)$ fatigue model may be obtained similarly. For a damage process, matching the order $O(\zeta^{-1})$ terms in (46):

$$\omega^o_{,t} + \omega^1_{,\tau} = \left(\frac{\theta^o}{\omega^o}\right)^\gamma (\theta^o_{,t} + \theta^1_{,\tau}) + \gamma\left(\frac{\theta^o}{\omega^o}\right)^\gamma \left(\frac{\theta^1}{\theta^o} - \frac{\omega^1}{\omega^o}\right)\theta^o_{,\tau} \tag{48}$$

where;

$$\theta^o_{,t} = \frac{\partial\theta^o}{\partial\upsilon^o}\upsilon^o_{,t}, \quad \text{and} \quad \theta^1_{,\tau} = \frac{\partial\theta^1}{\partial\upsilon^o}\upsilon^o_{,\tau} + \frac{\partial\theta^1}{\partial\upsilon^1}\upsilon^1_{,\tau} \tag{49}$$

To solve for (48), we assume the following decomposition for the higher order damage term, ω^1:

$$\omega^1 = \left(\frac{\theta^o}{\omega^o}\right)^\gamma \theta^1 \tag{50}$$

Substituting (50) into (48) the higher order terms of the above equation are eliminated. Furthermore, in the absence of micro-chronological loading, (48) reduces to:

$$\tilde{\omega}^o_{,t} = \left(\frac{\theta^o}{\tilde{\omega}^o}\right)^\gamma \frac{\partial\theta^o}{\partial\tilde{\upsilon}^o}\tilde{\upsilon}^o_{,t} \tag{51}$$

where $\tilde{\upsilon}^o \equiv \tilde{\upsilon}^o(\langle\boldsymbol{\varepsilon}^o\rangle)$ has the same form as in (13).

Various orders of the damage equivalent strain may be obtained by the asymptotic expansion of (13). Exploiting the symmetry of $\hat{\mathbf{L}}$:

$$\begin{aligned}\left[\upsilon^o + \zeta\upsilon^1 + O(\zeta^2)\right]^2 = \frac{1}{2}&\left[\mathbf{F}^o\hat{\boldsymbol{\varepsilon}}^o + \zeta(\mathbf{F}^o\hat{\boldsymbol{\varepsilon}}^1 + \mathbf{F}^1\hat{\boldsymbol{\varepsilon}}^o) + O(\zeta^2)\right]\hat{\mathbf{L}}\cdot \\ &\left[\mathbf{F}^o\hat{\boldsymbol{\varepsilon}}^o + \zeta(\mathbf{F}^o\hat{\boldsymbol{\varepsilon}}^1 + \mathbf{F}^1\hat{\boldsymbol{\varepsilon}}^o) + O(\zeta^2)\right]\end{aligned} \tag{52}$$

The first two orders of υ^ζ may then be given as:

$$O(1): \quad \upsilon^o = \sqrt{\frac{1}{2}\left(\mathbf{F}^o\hat{\boldsymbol{\varepsilon}}^o\right)\hat{\mathbf{L}}\left(\mathbf{F}^o\hat{\boldsymbol{\varepsilon}}^o\right)} \tag{53a}$$

$$O(\zeta): \quad \upsilon^1 = \frac{1}{2\upsilon^o}\left(\mathbf{F}^o\hat{\boldsymbol{\varepsilon}}^1 + \mathbf{F}^1\hat{\boldsymbol{\varepsilon}}^o\right)\hat{\mathbf{L}}\left(\mathbf{F}^o\hat{\boldsymbol{\varepsilon}}^1 + \mathbf{F}^1\hat{\boldsymbol{\varepsilon}}^o\right) \tag{53b}$$

The diagonal components of the strain weighting matrix, $\mathbf{F}^\zeta$, may be expressed in terms of vectors $\mathbf{h}^m$. For instance:

$$\mathbf{h}^o = \frac{1}{2} + \frac{1}{\pi}\arctan\left[a_1(\hat{\boldsymbol{\varepsilon}}^o - a_2)\right], \qquad \mathbf{h}^1 = \frac{\hat{\boldsymbol{\varepsilon}}^1/\pi}{1 + \left(a_1\hat{\boldsymbol{\varepsilon}}^o - a_2\right)^2} \tag{54}$$

Expressions for θ^m can be obtained by the asymptotic expansion of (11) (when $\upsilon^o \geq \upsilon_{ini}$, and $\upsilon^m \geq 0$):

$$\theta^o + \zeta\theta^1 + O(\zeta^2) = \frac{\arctan\left[\alpha\left(\frac{\upsilon^o + \zeta\upsilon^1 + O(\zeta^2) - \upsilon_{ini}}{\upsilon_o}\right) - \beta\right] + \arctan\beta}{\frac{\pi}{2} + \arctan\beta} \tag{55}$$

Matching the equal order terms in (55):

$$O(1): \quad \theta^o = \frac{\arctan\left[\alpha\left(\frac{\langle\upsilon^o - \upsilon_{ini}\rangle_+}{\upsilon_o}\right) - \beta\right] + \arctan\beta}{\frac{\pi}{2} + \arctan\beta} \tag{56a}$$

$$O(\zeta): \quad \theta^1 = \left(\frac{\alpha\upsilon_o}{\frac{\pi}{2} + \arctan(\beta)}\right) \frac{\upsilon^1}{\upsilon_o^2 + [\alpha(\upsilon^o - \upsilon_{ini}) - \beta\upsilon_o]^2} \tag{56b}$$

The higher order terms of υ^ζ, $\mathbf{h}^\zeta$ and θ^ζ may be evaluated using a similar algebra.

The corresponding equilibrium equation, initial and boundary conditions of order $O(1)$ macro-chronological IBVP are obtained by averaging (30, 32-34) over one load cycle using (35). The macro-chronological problem may then be posed as follows:

Equilibrium equation:	$\nabla \cdot \langle\boldsymbol{\sigma}^o\rangle + \langle\mathbf{b}\rangle(\mathbf{x},t) = \mathbf{0}$	on $\Omega \times (0,t_o)$	(57a)
Constitutive equation:	$\langle\boldsymbol{\sigma}^o\rangle_{,t} = (1 - \tilde{\omega}^o - \Lambda^o(\mathbf{x},t,\tau_1))\,\mathbf{L} : \langle\boldsymbol{\varepsilon}^o\rangle_{,t} - \left(\tilde{\omega}^o_{,t} + \Lambda^o_{,t}(\mathbf{x},t,\tau_1)\right)\mathbf{L} : \langle\boldsymbol{\varepsilon}^o\rangle$	on $\Omega \times (0,t_o)$	(57b)
Initial condition:	$\langle\mathbf{u}^o\rangle(\mathbf{x},t=0) = \tilde{\mathbf{u}}$	on Ω	(57c)
Boundary conditions:	$\langle\mathbf{u}^o\rangle = \langle\bar{\mathbf{u}}\rangle(\mathbf{x},t)$	on $\Gamma_u \times (0,t_o)$	(57d)
	$\langle\boldsymbol{\sigma}^o\rangle\mathbf{n} = \langle\mathbf{f}\rangle(\mathbf{x},t)$	on $\Gamma_f \times (0,t_o)$	(57e)

The equilibrium equation, initial and boundary conditions of the micro-chronological problem may be obtained by subtracting those of the macro-chronological problem from (30, 32-34), respectively. The micro-chronological IBVP of order $O(1)$ at a given instant of slow time coordinate, t, may then be posed as follows:

Equilibrium equation:	$\nabla \cdot \boldsymbol{\Phi}^o + \mathbf{b} - \langle\mathbf{b}\rangle = \mathbf{0}$	on $\Omega \times (0,\tau_o)$	(58a)
Constitutive equation:	$\boldsymbol{\Phi}^o_{,\tau} = (1 - \Lambda^o)\,\mathbf{L} : \boldsymbol{\Psi}^o_{,\tau} - \Lambda^o_{,\tau}\mathbf{L} : \boldsymbol{\Psi}^o - \tilde{\omega}^o\mathbf{L} : \boldsymbol{\Psi}^o_{,\tau} - \Lambda^o_{,\tau}\mathbf{L} : \langle\boldsymbol{\varepsilon}^o\rangle$	on $\Omega \times (0,\tau_o)$	(58b)
Initial condition:	$\boldsymbol{\chi}^o = \mathbf{0}$	on Ω	(58c)
Boundary conditions:	$\boldsymbol{\chi}^o = \bar{\mathbf{u}}(\mathbf{x},t,\tau) - \langle\bar{\mathbf{u}}\rangle$	on $\Gamma_u \times (0,\tau_o)$	(58d)
	$\boldsymbol{\Phi}^o\mathbf{n} = \mathbf{f} - \langle\mathbf{f}(\mathbf{x},t,\tau)\rangle$	on $\Gamma_f \times (0,\tau_o)$	(58e)

The constitutive equations of the micro- and macro-chronological problems clearly show a two-way coupling. Hence, the micro-chronological initial boundary value problem defined by (38), (58c-58e) has to be solved at every time step of the macro-chronological problem. Computational aspects and solution procedures of the order $O(1)$ IBVPs are discussed in the following section.

The higher order initial boundary value problems may be obtained using a scheme similar to the formulation of order $O(1)$ problems. The macro-chronological IBVP of order $O(\zeta^{m+1})$ is given as:

$$\text{Equilibrium equation:} \qquad \nabla \cdot \langle \boldsymbol{\sigma}^{m+1} \rangle = \mathbf{0} \qquad \text{on } \Omega \times (0, t_o) \tag{59a}$$

$$\begin{aligned} \text{Constitutive equation:} \qquad \langle \boldsymbol{\sigma}^{m+1} \rangle_{,t} = \mathbf{L} : \langle \boldsymbol{\varepsilon}^{m+1} \rangle_{,t} - \sum_{s=0}^{m+1} \omega^s (\mathbf{x}, t, \tau_1) \mathbf{L} : \langle \boldsymbol{\varepsilon}^{m+1-s} \rangle_{,t} - \\ \sum_{s=0}^{m+1} \omega^s_{,t} (\mathbf{x}, t, \tau_1) \mathbf{L} : \langle \boldsymbol{\varepsilon}^{m+1-s} \rangle \quad \text{on } \Omega \times (0, t_o) \end{aligned} \tag{59b}$$

where $\omega^m (\mathbf{x}, t, \tau_1) = \tilde{\omega}^m + \Lambda^m (\mathbf{x}, t, \tau_1)$. Initial and boundary conditions for higher order macro-chronological problems are trivial.

The micro-chronological IBVP of order $O(\zeta^{m+1})$ at a given instant of slow time coordinate, t, is expressed as:

$$\text{Equilibrium equation:} \qquad \nabla \cdot \boldsymbol{\Phi}^{m+1} = \mathbf{0} \qquad \text{on } \Omega \times (0, \tau_o) \tag{60a}$$

$$\begin{aligned} \text{Constitutive equation:} \qquad \boldsymbol{\Phi}^{m+1}_{,\tau} = \mathbf{L} : \boldsymbol{\Psi}^{m+1}_{,\tau} - \sum_{s=0}^{m+1} (\tilde{\omega}^s + \Lambda^s) \mathbf{L} : \boldsymbol{\Psi}^{m+1-s}_{,\tau} - \\ \sum_{s=0}^{m+1} \Lambda^s_{,\tau} \mathbf{L} : \boldsymbol{\Psi}^{m+1-s} - \sum_{s=0}^{m+1} \Lambda^s_{,\tau} \mathbf{L} : \langle \boldsymbol{\varepsilon}^{m+1-s} \rangle \quad \text{on } \Omega \times (0, \tau_o) \end{aligned} \tag{60b}$$

Similar to the macro-chronological problem, the initial and boundary conditions are trivial. The higher order problems defined in (59) and (60) are fully coupled in addition to the contributions from the lower order terms.

In this section, a two scale asymptotic analysis was conducted to resolve the temporal scales for the failure processes with accumulation of distributed damage. Asymptotic analysis of the failure mechanisms with propagation of macrocracks is somewhat similar and will be skipped.

4 Computational issues

Finite element models of order $O(1)$ micro- and macro-chronological problems were implemented and details of the implementation are discussed herein. The constitutive equations of the micro- and macro-chronological problems ((58b) and (57b), respectively) were shown to be coupled in the previous section. In this study, these two problems where evaluated in a staggered manner. Figure 2 displays a sketch of the general structure of the algorithm. An external batch file controls the execution of the algorithm which in turn invokes a conventional finite element program. The entire micro-chronological IBVP, which represents a single cycle of loading, is evaluated prior to the execution of each time step of the macro-chronological problem. The state variable information transfer between the two problems is conducted through external files stored on a hard disk. This specific structure of the algorithm is selected to accommodate the use of commercial finite element packages along with the appropriate user supplied subroutines (e.g., UMAT in ABAQUS).

4.1 Stress update procedure

4.1.1 Micro-chronological problem

Given: Strain and stress tensors, ${}_{\tau}\boldsymbol{\Psi}^{o}$ and ${}_{\tau}\boldsymbol{\Phi}^{o}$, respectively; micro-chronological strain increment, $\delta\boldsymbol{\Psi}^{o}$, micro-chronological damage variable, ${}_{\tau}\Lambda^{o}$, at the beginning of the time step; macro-

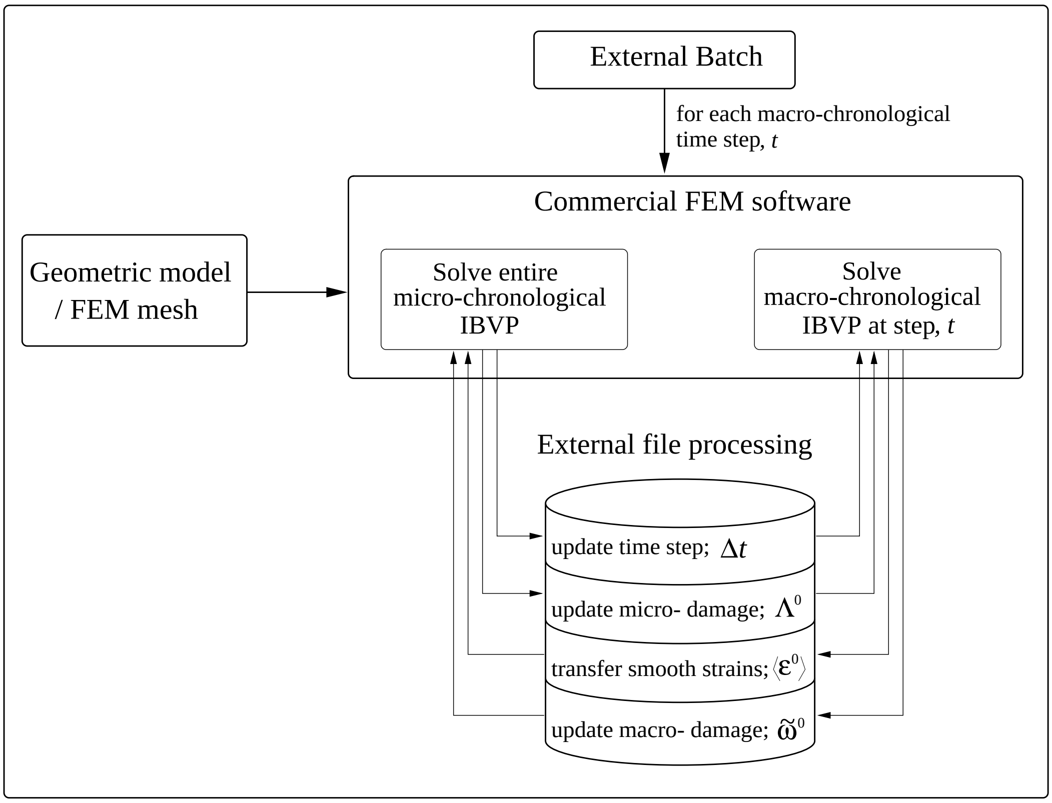

Figure 2: Schematic of the program architecture for the multi-scale fatigue life prediction analysis.

chronological strain tensor and damage variable, $\langle \boldsymbol{\varepsilon}^o \rangle$ and $\tilde{\omega}^o$, respectively. ${}_{\tau}(\cdot)$ and ${}_{\tau+\delta\tau}(\cdot)$ denote the state of field variables at the beginning of the time step and their current values, respectively. For simplicity we will often omit the subscript for the current values; i.e., $(\cdot) \equiv {}_{\tau+\delta\tau}(\cdot)$.

Compute: Stress and strain tensors, ${}_{\tau+\delta\tau}\boldsymbol{\Psi}^o$ and ${}_{\tau+\delta\tau}\boldsymbol{\Phi}^o$, respectively, and micro-chronological strain induced damage variable, ${}_{\tau+\delta\tau}\Lambda^o$.

The stress update procedure for the micro-chronological problem is outlined below:

1. Update strain tensor: $\boldsymbol{\Psi}^o = {}_{\tau}\boldsymbol{\Psi}^o + \delta\boldsymbol{\Psi}^o$

2. Compute the current total strains, $\boldsymbol{\varepsilon}^o = {}_{\tau+\delta\tau}\boldsymbol{\Psi}^o + \langle \boldsymbol{\varepsilon}^o \rangle$, and project the total strain tensor to the principle frame.

3. Compute the damage equivalent strain, ${}_{\tau+\delta\tau}\upsilon^o$, using (53a) along with $\hat{\mathbf{L}}$ and $\hat{\boldsymbol{\varepsilon}}^o$.

4. In case ${}_{\tau+\delta\tau}\upsilon^o > {}_{\tau}\upsilon^o$ and ${}_{\tau+\delta\tau}\upsilon^o \geq \upsilon_{ini}$, update, Λ^o using (47). An implicit backward Euler algorithm was used to integrate the fatigue damage law:

$$\Xi \equiv {}_{\tau+\delta\tau}\Lambda^o - {}_{\tau}\Lambda^o - {}_{\tau+\delta\tau}\left(\frac{\theta^o}{\Lambda^o + \tilde{\omega}^o}\right)^{\gamma} {}_{\tau+\delta\tau}\left(\frac{\partial\theta^o}{\partial\upsilon^o}\right)\left({}_{\tau+\delta\tau}\upsilon^o - {}_{\tau}\upsilon^o\right) = 0 \tag{61}$$

where,

$$\frac{\partial\theta^o}{\partial\upsilon^o} = \left(\frac{\alpha\upsilon_o}{\frac{\pi}{2} + \arctan\beta}\right)\frac{1}{(\upsilon_o)^2 + [\alpha(\upsilon^o - \upsilon_{ini}) - \beta\upsilon_o]^2} \tag{62}$$

The above equation was solved for ${}_{\tau+\delta\tau}\Lambda^{\mathrm{o}}$ using Newton method:

$$ {}^{i+1}\Lambda^{\mathrm{o}} = {}^{i}\Lambda^{\mathrm{o}} - \left[\left(\frac{\partial \Xi}{\partial \Lambda^{\mathrm{o}}} \right)^{-1} \Xi \right] \Bigg|_{{}^{i}\Lambda^{\mathrm{o}}} \tag{63} $$

where,

$$ \frac{\partial \Xi}{\partial \Lambda^{\mathrm{o}}} = 1 + \left(\frac{\gamma}{\Lambda^{\mathrm{o}} + \tilde{\omega}^{\mathrm{o}}} \right) \left(\frac{\theta^{\mathrm{o}}}{\Lambda^{\mathrm{o}} + \tilde{\omega}^{\mathrm{o}}} \right)^{\gamma} \left(\frac{\partial \theta^{\mathrm{o}}}{\partial \upsilon^{\mathrm{o}}} \right) \left({}_{\tau+\delta\tau}\upsilon^{\mathrm{o}} - {}_{\tau}\upsilon^{\mathrm{o}} \right) \tag{64} $$

5. In case ${}_{\tau+\delta\tau}\upsilon^{\mathrm{o}} \leq {}_{\tau}\upsilon^{\mathrm{o}}$ or ${}_{\tau+\delta\tau}\upsilon^{\mathrm{o}} < \upsilon_{ini}$, no damage is accumulated at the current step:

$$ {}_{\tau+\delta\tau}\Lambda^{\mathrm{o}} = {}_{\tau}\Lambda^{\mathrm{o}} \tag{65} $$

6. Compute the stress increment $\delta\mathbf{\Phi}^{\mathrm{o}}$ using (38) and update stress tensor:

$$ {}_{\tau+\delta\tau}\mathbf{\Phi}^{\mathrm{o}} = {}_{\tau}\mathbf{\Phi}^{\mathrm{o}} + \delta\mathbf{\Phi}^{\mathrm{o}} \tag{66} $$

4.1.2 Macro-chronological problem

Given: Strain and stress tensors, ${}_{t}\langle\boldsymbol{\varepsilon}^{\mathrm{o}}\rangle$ and ${}_{t}\langle\boldsymbol{\sigma}^{\mathrm{o}}\rangle$, respectively; macro-chronological strain increment, $\Delta\langle\boldsymbol{\varepsilon}^{\mathrm{o}}\rangle$, micro- and macro-chronological strain induced damage variables, ${}_{t}\Lambda^{\mathrm{o}}(\tau_1)$ and ${}_{t}\tilde{\omega}^{\mathrm{o}}$, respectively; macro-chronological time step, Δt, which is computed adaptively. ${}_{t}(\cdot)$ and ${}_{t+\Delta t}(\cdot)$ denote the state of field variables at the beginning of the time step and their current values, respectively. Similar to the previous section, quantities without left subscript denote the current values; i.e., $(\cdot) \equiv {}_{t+\Delta t}(\cdot)$.

Compute: Stress and strain tensors, ${}_{t+\Delta t}\langle\boldsymbol{\varepsilon}^{\mathrm{o}}\rangle$ and ${}_{t+\Delta t}\langle\boldsymbol{\sigma}^{\mathrm{o}}\rangle$, respectively, and current micro- and macro-chronological strain induced damage variables, ${}_{t+\Delta t}\Lambda^{\mathrm{o}}(\tau_1)$ and ${}_{t+\Delta t}\tilde{\omega}^{\mathrm{o}}$, respectively.

The stress update procedure for the macro-chronological problem is summarized below:

1. Update strain tensor: $\langle\boldsymbol{\varepsilon}^{\mathrm{o}}\rangle = {}_{t}\langle\boldsymbol{\varepsilon}^{\mathrm{o}}\rangle + \Delta\langle\boldsymbol{\varepsilon}^{\mathrm{o}}\rangle$

2. Update the micro-chronological strain induced damage variable. In this study, Λ^{o} is taken to be a piecewise linear function of the slow time coordinate, t:

$$ {}_{t+\Delta t}\Lambda^{\mathrm{o}}(\tau_1) = {}_{t}\Lambda^{\mathrm{o}}(\tau_1) + m^{\mathrm{o}}\Delta t \tag{67} $$

   where $m^{\mathrm{o}} = [{}_{t}\Lambda^{\mathrm{o}}(\tau_{\mathrm{o}}) - {}_{t}\Lambda^{\mathrm{o}}(0)]/\tau_{\mathrm{o}}$, is the rate of micro-chronological damage growth and is computed during the evaluation of micro-chronological problem.

3. Compute the principal components of the macro-chronological strains, $\langle\boldsymbol{\varepsilon}^{\mathrm{o}}\rangle$.

4. Compute the damage equivalent strain ${}_{t+\Delta t}\tilde{\upsilon}^{\mathrm{o}}$ using an Euler Backward algorithm and (51), along with $\hat{\mathbf{L}}$ and $\langle\hat{\boldsymbol{\varepsilon}}^{\mathrm{o}}\rangle$.

5. In case, ${}_{t+\Delta t}\tilde{\upsilon}^{\mathrm{o}} > {}_{t}\tilde{\upsilon}^{\mathrm{o}}$ and ${}_{t+\Delta t}\tilde{\upsilon}^{\mathrm{o}} \geq \upsilon_{ini}$, update macro-chronological damage variable, $\tilde{\omega}^{\mathrm{o}}$ using a similar implicit backward Euler algorithm outlined in the stress update procedure of the micro-chronological problem, by replacing fast time coordinate τ with t, and Λ^{o} with $\tilde{\omega}^{\mathrm{o}}$ (except for the term with power, γ, where Λ^{o} is omitted).

6. In case ${}_{t+\Delta t}\tilde{\upsilon}^{\mathrm{o}} \leq {}_{t}\tilde{\upsilon}^{\mathrm{o}}$ or ${}_{t+\Delta t}\tilde{\upsilon}^{\mathrm{o}} < \upsilon_{ini}$, no damage is accumulated at the current step:

$$ {}_{t+\Delta t}\tilde{\omega}^{\mathrm{o}} = {}_{t}\tilde{\omega}^{\mathrm{o}} \tag{68} $$

7. Compute the stress increment $\Delta\langle\boldsymbol{\sigma}^{\mathrm{o}}\rangle$ using (42) and update stress tensor:

$$ {}_{t+\Delta t}\langle\boldsymbol{\sigma}^{\mathrm{o}}\rangle = {}_{t}\langle\boldsymbol{\sigma}^{\mathrm{o}}\rangle + \Delta\langle\boldsymbol{\sigma}^{\mathrm{o}}\rangle \tag{69} $$

4.2 Consistent tangent stiffness

The constitutive equations of the first order micro- and macro-chronological IBVPs were presented in the previous sections ((38) and (42), respectively). The consistent tangent stiffness matrices are developed herein.

4.2.1 Micro-chronological problem

Constitutive equation of the micro-chronological problem may be rewritten in the following form:

$$ \boldsymbol{\Phi}^{\mathrm{o}}_{,\tau} = (1 - \Lambda^{\mathrm{o}} - \tilde{\omega}^{\mathrm{o}})\,\mathbf{L} : \boldsymbol{\Psi}^{\mathrm{o}}_{,\tau} - \Lambda^{\mathrm{o}}_{,\tau}\mathbf{L} : (\boldsymbol{\Psi}^{\mathrm{o}} + \langle\boldsymbol{\varepsilon}^{\mathrm{o}}\rangle) \tag{70} $$

In the case of an elastic process, ($\upsilon^{\mathrm{o}} < \upsilon_{ini}$) or unloading ($\langle\upsilon^{\mathrm{o}}_{,\tau}\rangle_{+} = 0$), no damage is accumulated ($\Lambda_{,\tau}$=0). Therefore, (70) reduces to:

$$ \boldsymbol{\Phi}^{\mathrm{o}}_{,\tau} = (1 - \Lambda^{\mathrm{o}} - \tilde{\omega}^{\mathrm{o}})\mathbf{L} : \boldsymbol{\Psi}^{\mathrm{o}}_{,\tau} \tag{71} $$

For a damage process (i.e., $\upsilon^{\mathrm{o}} \geq \upsilon_{ini}$ and $\langle\upsilon^{\mathrm{o}}_{,\tau}\rangle_{+} > 0$), $\Lambda^{\mathrm{o}}_{,\tau}$ may be expressed in terms of micro-chronological strains, $\boldsymbol{\Psi}^{\mathrm{o}}_{,\tau}$, using the cumulative damage law defined in (47):

$$ \Lambda^{\mathrm{o}}_{,\tau} = \mathbf{S} : \boldsymbol{\Psi}^{\mathrm{o}}_{,\tau} \tag{72} $$

where $\mathbf{S}$ is a second order tensor. Details of the derivation of (72) is presented in Appendix A. Inserting (72) into (70) and rearranging the terms yields:

$$ \boldsymbol{\Phi}^{\mathrm{o}}_{,\tau} = \mathbf{P} : \boldsymbol{\Psi}^{\mathrm{o}}_{,\tau} \tag{73} $$

and;

$$ \mathbf{P} = \mathbf{L} : [(1 - \Lambda^{\mathrm{o}} - \tilde{\omega}^{\mathrm{o}})\mathbf{I} - (\boldsymbol{\Psi}^{\mathrm{o}} + \langle\boldsymbol{\varepsilon}^{\mathrm{o}}\rangle) \otimes \mathbf{S}] \tag{74} $$

in which $\mathbf{P}$ is the tangent stiffness tensor for a damage process in the micro-chronological scale, and, $\otimes$ represents a tetradic product of two second order tensors (e.g., $A_{ijkl} = B_{ij}C_{kl}$ for cartesian coordinate system).

4.2.2 Macro-chronological problem

The constitutive equation of the first order macro-chronological problem may be written in the following form:

$$ \langle\boldsymbol{\sigma}^{\mathrm{o}}\rangle_{,t} = (1 - \omega^{\mathrm{o}}(\mathbf{x}, t, \tau_1))\,\mathbf{L} : \langle\boldsymbol{\varepsilon}^{\mathrm{o}}\rangle_{,t} - \omega^{\mathrm{o}}_{,t}(\mathbf{x}, t, \tau_1)\,\mathbf{L} : \langle\boldsymbol{\varepsilon}^{\mathrm{o}}\rangle \tag{75} $$

In the case of an elastic process and unloading in the slow time scale, $\omega^{\mathrm{o}}_{,t}(\mathbf{x}, t, \tau_1) = 0$ and constitutive equation reduces to:

$$ \langle\boldsymbol{\sigma}^{\mathrm{o}}\rangle_{,t} = (1 - \omega^{\mathrm{o}}(\mathbf{x}, t, \tau_1))\,\mathbf{L} : \langle\boldsymbol{\varepsilon}^{\mathrm{o}}\rangle_{,t} \tag{76} $$

When the macro-chronological loading is at the inelastic range (damage process):

$$\omega^{o}_{,t}(\mathbf{x},t,\tau_1) = \mathbf{R} : \langle \boldsymbol{\varepsilon}^{o} \rangle_{,t} \tag{77}$$

where $\mathbf{R}$ is a second order tensor. The derivation of $\mathbf{R}$ is much similar to the derivation of $\mathbf{S}$, and details are presented in Appendix A. Substituting (77) into (75) and rearranging the terms yields:

$$\langle \boldsymbol{\sigma}^{o} \rangle_{,t} = \mathbf{K} : \langle \boldsymbol{\varepsilon}^{o} \rangle_{,t} \tag{78}$$

and,

$$\mathbf{K} = \mathbf{L} : \left[(1 - \omega^{o}(\mathbf{x},t,\tau_1))\,\mathbf{I} - \langle \boldsymbol{\varepsilon}^{o} \rangle \otimes \mathbf{R} \right] \tag{79}$$

where $\mathbf{K}$ is the tangent stiffness tensor for a damage process in the macro-chronological scale.

4.3 Evaluation of macro-chronological step size, Δt

The accuracy of the proposed two-scale evaluation of fatigue damage evolution depends on the size of the time incrementation of the macro-chronological problem. Selection of an appropriate time step size is a trade-off between the resolution of the damage variable or the crack growth rate, and computational cost. We address this problem by employing an adaptive Modified Euler algorithm with maximum damage control. By this approach, the time step for the macro-scale problem is partly computed during the micro-chronological analysis.

Let $\Lambda^{o}|_{t}$ be the micro-chronological strain induced damage variable, at slow time instant, t. The increment of Λ^{o} per one load-cycle may be expressed as:

$$\delta\Lambda^{o}|_{N_t} = \Lambda^{o}|_{N_t+1} - \Lambda^{o}|_{N_t} \tag{80}$$

where N_t denotes the load cycle number; $\Lambda^{o}|_{N_t} = \Lambda^{o}(t,0)$ and $\Lambda^{o}|_{N_t+1} = \Lambda^{o}(t,\tau_o)$ are the state of damage variable at the beginning and end of the micro-chronological problem, respectively. Using the modified Euler integrator [23], micro-chronological damage variable, $\Lambda^{o}|_{N_t+\Delta N_t}$, at load cycle, $N_t + \Delta N_t$, may be defined as:

$$\Lambda^{o}|_{(N_t+\Delta N_t;\Delta N_t)} = \Lambda^{o}|_{N_t} + \frac{\Delta N_t}{2}\left(\delta\Lambda^{o}|_{N_t} + \delta\Lambda^{o}|_{N_t+\Delta N_t}\right) \tag{81}$$

where δ and Δ refers to the quantities related to the micro- and macro-chronological scales, respectively. $\delta\Lambda^{o}|_{N_t+\Delta N_t}$ may be obtained by substituting $N_t + \Delta N_t$ for N_t in (80):

$$\delta\Lambda^{o}|_{N_t+\Delta N_t} = \Lambda^{o}|_{N_t+\Delta N_t+1} - \Lambda^{o}|_{N_t+\Delta N_t} \tag{82}$$

where a first approximation of $\Lambda^{o}|_{N_t+\Delta N_t-1}$ is obtained using a forward Euler scheme:

$$\Lambda^{o}|_{N_t+\Delta N_t} = \Lambda^{o}|_{N_t} + \Delta N_t \delta\,\Lambda^{o}|_{N_t} \tag{83}$$

The value of macro-chronological step size Δt is a linear function of ΔN_t ($\Delta t = \tau_o \Delta N_t$), and ΔN_t is selected heuristically to control accuracy. For instance, the value of ΔN_t must be sufficiently small when the rate of increase of Λ^{o} or the crack length is high, and vice versa. This condition may be achieved by constraining the maximum damage accumulation within the macro-chronological time step, Δt at all integration points:

$$\Delta N_t = \mathrm{int}\left[\frac{\delta\Lambda^{o}_{all}}{\|\,\delta\Lambda^{o}|_{N_t}\,\|_{k}}\right]; \quad k = 1 \ \text{or} \ \infty \tag{84}$$

in which $\delta\Lambda^{o}_{all}$ is the maximum allowable accumulation of damage within a micro-chronological problem.

The adaptive scheme for the macro-chronological step size evaluation is summarized below:

Prior to the t^{th} step of the macro-chronological problem:

1. Carry out the micro-chronological IBVP, as described in Section (4.1.1) to obtain $\Lambda^{o}|_{N_t+1}$. Compute the change in damage variable per cycle, $\delta\Lambda^{o}|_{N_t}$ using (80) at each integration point of the mesh.

2. Compute the initial block size ΔN_t using (84).

3. Set the block size to ΔN_t and compute $\Lambda^{o}|_{(N_t+\Delta N_t;\Delta N_t)}$ using modified Euler algorithm defined in (80-83).

4. Set the block size to $\Delta N_t/2$ and compute $\Lambda^{o}|_{(N_t+\Delta N_t;\Delta N_t/2)}$ by two successive invocation of the modified Euler algorithm (note that steps 3 and 4 require the evaluation of micro-chronological model three additional times prior to every macro-chronological step).

5. Compute maximum error at each integration step and compare to the predefined error tolerance e^{tol}_{k} such that:

$$\| \Lambda^{o}|_{(N_t+\Delta N_t;\Delta N_t)} - \Lambda^{o}|_{(N_t+\Delta N_t;\Delta N_t/2)} \|_k \leq e^{tol}_{k}; \quad k=1 \text{ or } \infty \tag{85}$$

   using the values computed at all integration points.

6. If (85) holds, set the macro-chronological problem step size at time t to $\Delta t = \tau_o \Delta N_t$ and set the micro-scale contribution of damage, $\Lambda^{o}|_{(N_t+\Delta N_t)} = \Lambda^{o}|_{(N_t+\Delta N_t;\Delta N_t/2)}$. Print damage information into external transfer files and exit adaptive algorithm. If (85) does not hold, set $\Delta N_t = \Delta N_t/2$ and go back to step 3.

Remark: An analogous adaptive algorithm can be applied in the macro-chronological problem to control the growth of the macro-chronological strain induced damage, $\tilde{\omega}^{o}$.

5 Numerical examples

5.1 Four-point bending beam

A four-point bending problem with a configuration defined in Fig. 3 is considered for analysis of fatigue failure mechanisms by accumulation of distributed damage. The beam is made of an isotropic brittle material. Microdefects are assumed to be homogeneously distributed along the beam and fatigue damage evolution law is applied to the entire geometry. The material properties used to conduct the numerical simulations are outlined in Table 1. Nodal loads are applied at the crossheads of the beam (Fig. 3):

$$\bar{f} = F_\tau \sin(\omega t) + F_t[1-\exp(-t/t_d)] \tag{86}$$

in which F_τ and F_t are the amplitudes of the periodic and smooth loads, respectively; ω is circular frequency; and t_d is a constant in the order of the characteristic length of the macro-chronological scale. The values used in our simulations are presented in Table 2.

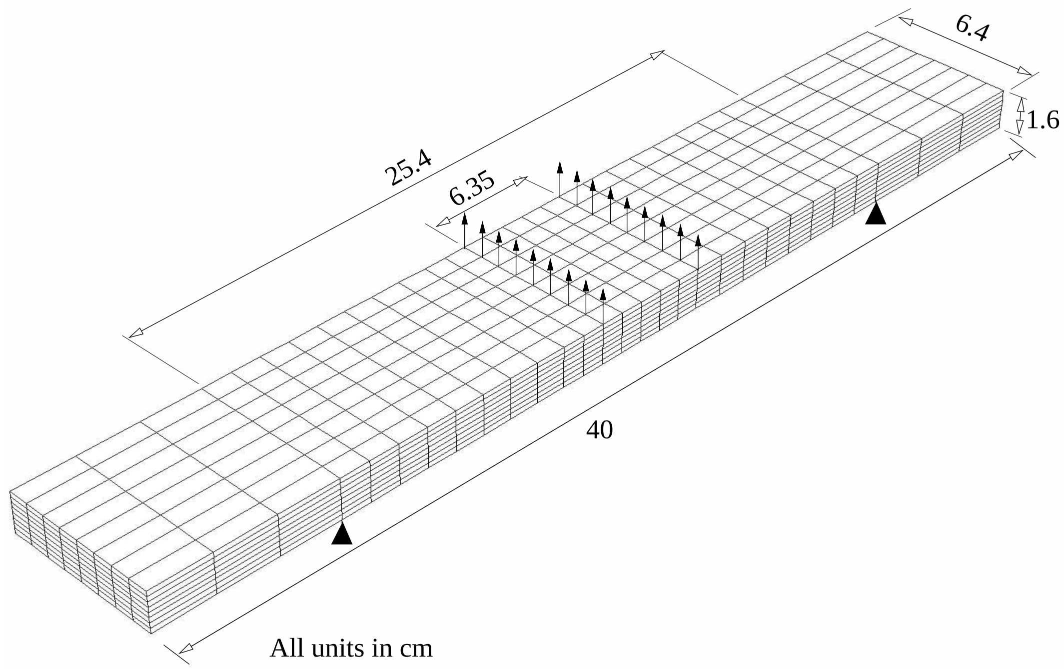

Figure 3: Configuration and the finite element mesh of 4-point bending beam model.

Table 1: Material properties used in 4-point bending beam analysis.

Material property	Value
Young's modulus, E	50 GPa
Poisson's ratio, ν	0.3
υ_o	0.05
υ_{ini}	0.0
α	8.2
β	10.2
γ	4.5
a_1	1e7
a_2	0.0

Figure 4 illustrates the evolution of damage variable, ω^o computed using the proposed adaptive multi-scale algorithm and cycle-by-cycle (reference solution) approach. In cycle-by-cycle approach, each cycle of the loading is resolved and evaluated by a direct numerical algorithm based on a backward Euler scheme. The depicted damage history is at an integration point at the mid-span of the mesh. Figures 5-7 show the damaged configurations of the beam for multi-scale and reference algorithms after 1000 load cycles. Stress, strain and damage variable histories revealed a close agreement between the proposed multi-scale and the reference solutions.

5.2 Beam under periodic loading

Failure evolution by propagation of macrocracks is investigated on a beam problem as shown in Fig. 8. Cohesive elements are placed at the midsection, and an initial flaw is introduced at the center bottom of the beam. The material properties used to conduct the numerical simulations are summarized in Table 3. Plane strain conditions are considered and the beam is subjected to

Table 2: Loading parameters used in 4-point bending beam analysis.

Loading parameter	Value
F_τ	4
F_t	35
ω	$20\ \pi$ rad/hr
t_d	3.2 hr

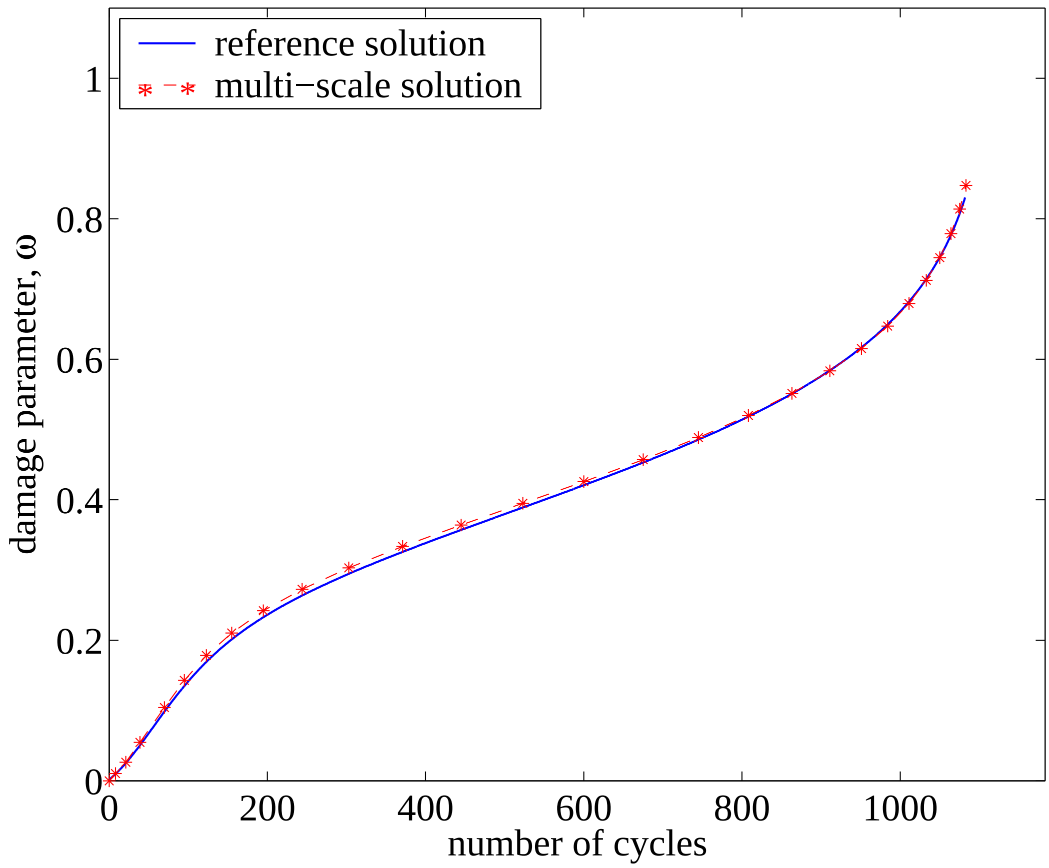

Figure 4: Fatigue damage accumulation at the midspan of the beam.

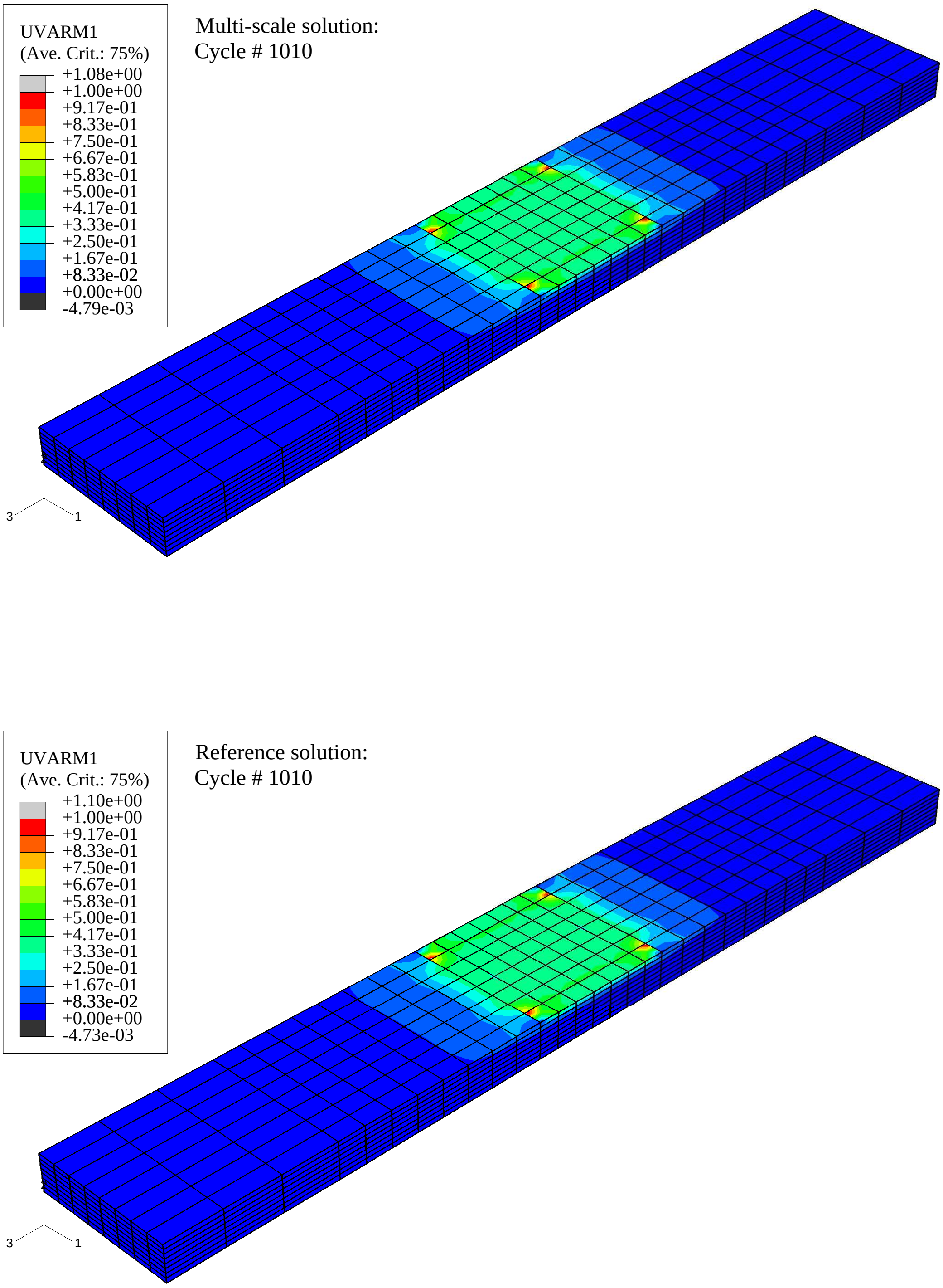

Figure 5: Damage distribution at the failure stage in the four-point bending beam problem.

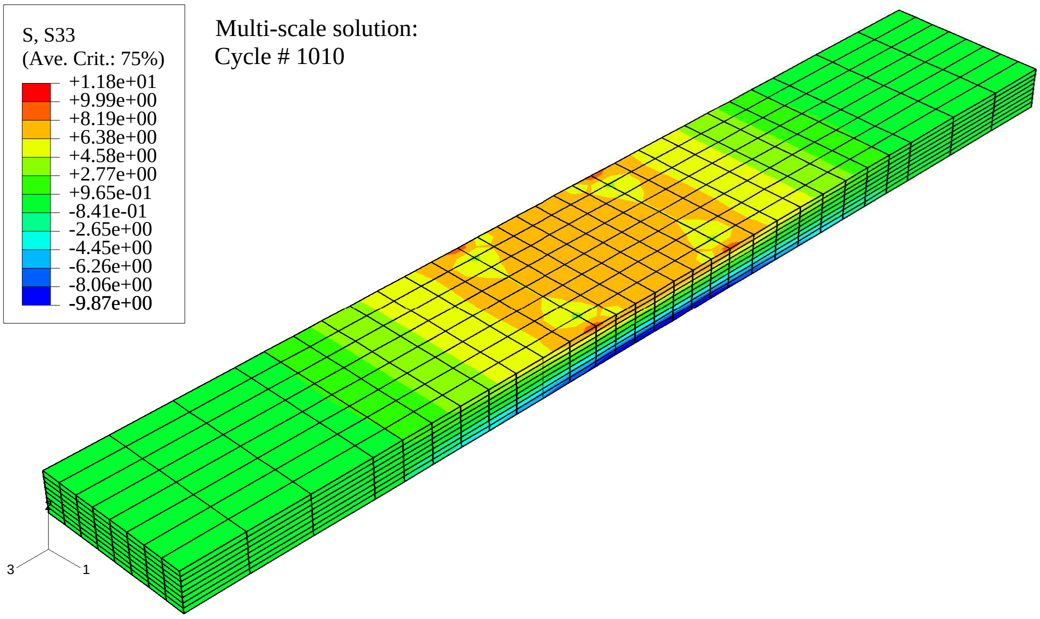

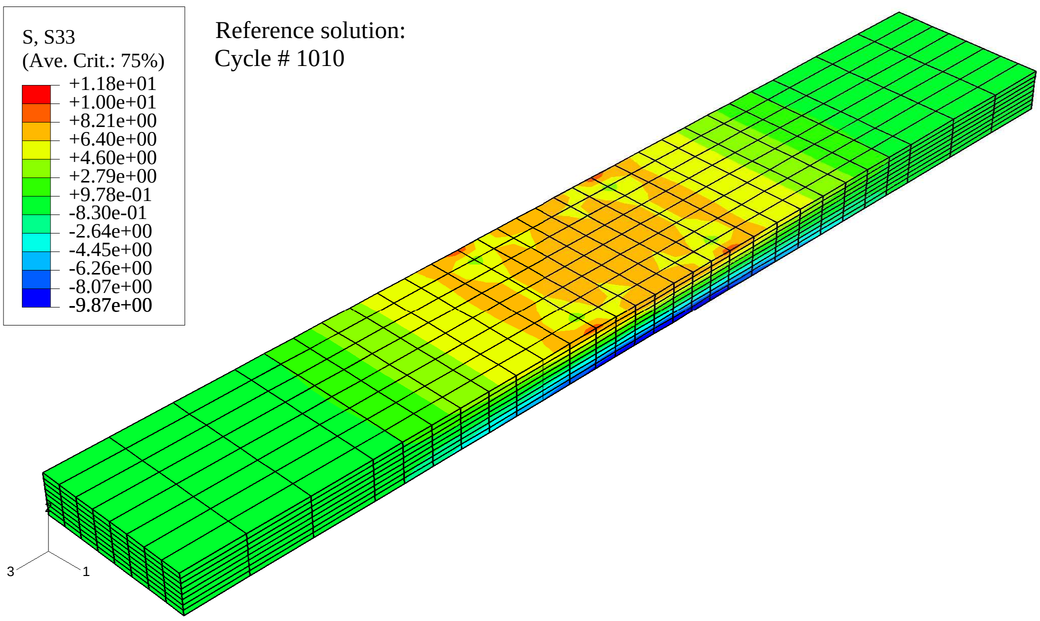

Figure 6: Stress distribution at the failure stage in the four-point bending beam problem.

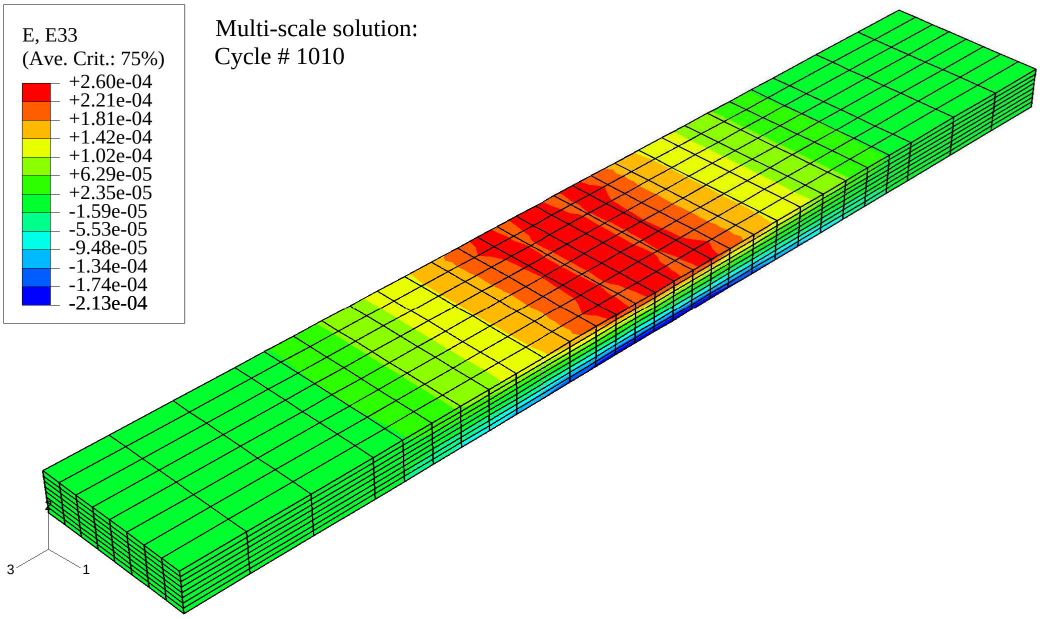

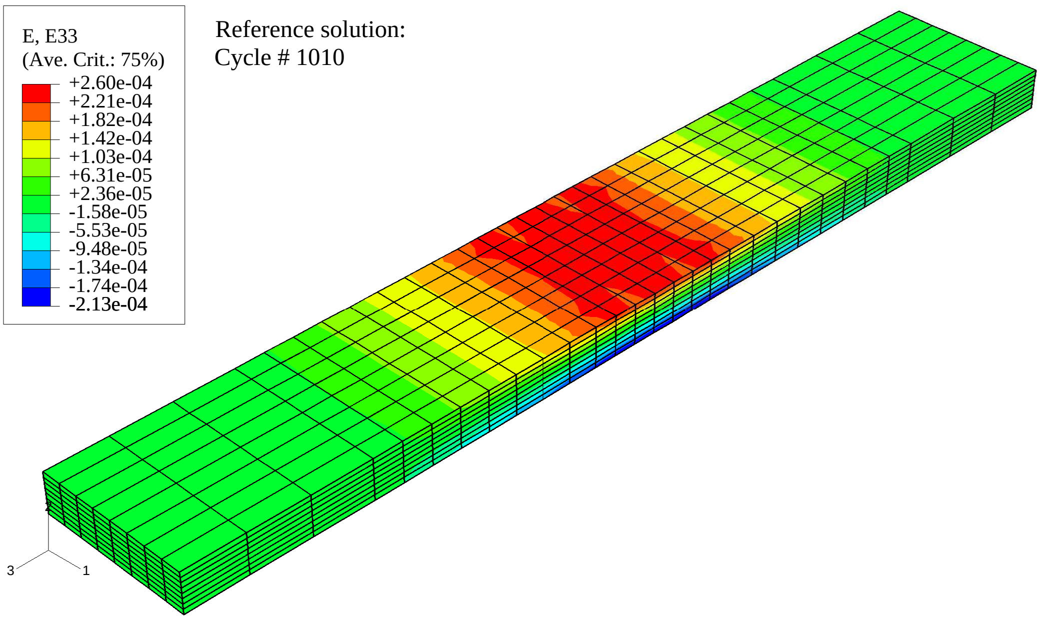

Figure 7: Strain distribution at the failure stage in the four-point bending beam problem.

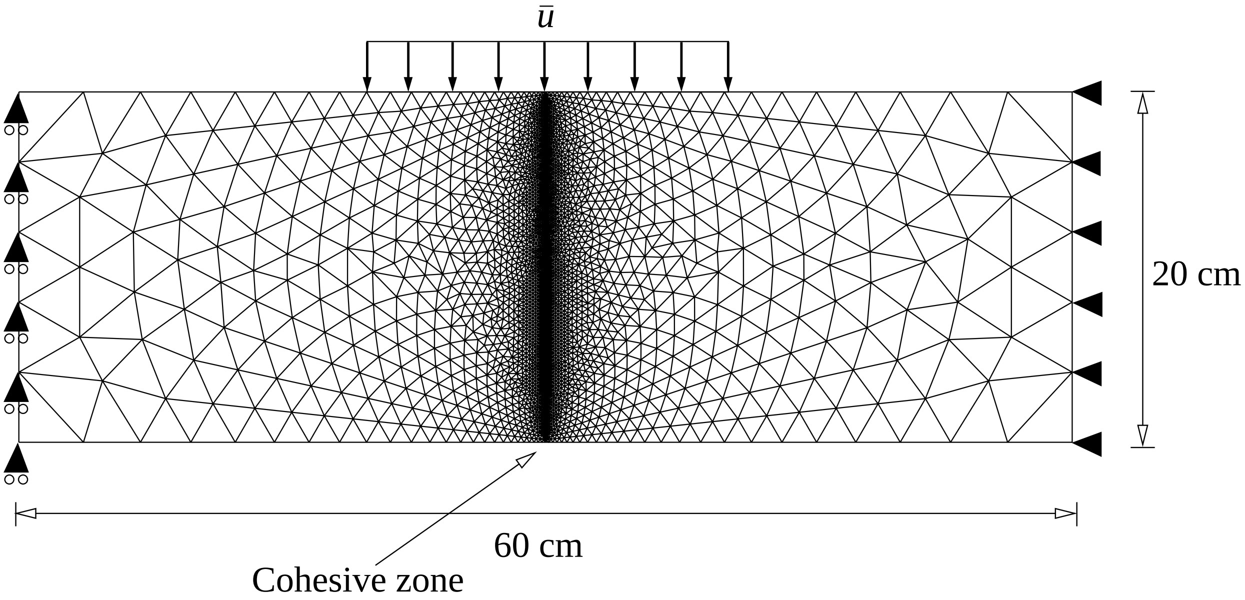

Figure 8: Configuration and the finite element mesh of the beam under periodic loading.

periodic displacements (Fig. 8):

$$\bar{u} = \frac{u_\tau}{2}\left(1 + \cos(\omega t - \pi)\right) \tag{87}$$

where u_τ is amplitude of the periodic prescribed displacements, and ω is circular frequency. The values used in our simulations are presented in Table 4.

Figure 9 illustrates a close agreement between the fatigue life curves evaluated using the proposed multiscale and the reference (cycle-by-cycle) approach. The stress distributions along the beam after 40,000 cycles (when the crack is 15 mm long) and after 150,000 cycles (when the crack is 33 mm long) are presented in Fig. 10. As can be observed from this figure, a compressive region develops along the path of the crack due to force redistribution along the beam. This compressive region causes the crack arrest shown in Fig. 9.

6 Acknowledgement

This work was supported by the Office of Naval Research through grant number N00014-97-1-0687. This support is gratefully acknowledged.

7 Conclusion

This paper presented a new multiscale approach to the prediction of structural fatigue life based on asymptotic analysis with multiple temporal scales. This approach attempts to resolve the scale disparity between the time span of the period of loading and life span of a structural component. The theory was developed to analyze the failure mechanisms with the accumulation of distributed damage, and propagation of macrocracks up to failure based on the assumption of small scale yielding. The effects of the plastic deformations near the crack tip will be addressed in a future publication. The proposed methodology was implemented using a commercial finite element package (ABAQUS) and validated against cycle-by-cycle approach.

Table 3: Material properties used in the beam under periodic loading example.

Material property (Γ_c)	Value
Young's modulus, E	5 GPa
Poisson's ratio, ν	0.3
υ_o	0.05
υ_{ini}	0.0
α	8.2
β	10.2
γ	4.5
a_1	1e7
a_2	0.0
w	0.0
Material property ($\Gamma \sim \Gamma_c$)	**Value**
Young's modulus, E	70 GPa
Poisson's ratio, ν	0.3

Table 4: Loading parameters used in the beam under periodic loading example.

Loading parameter	Value
u_τ	2.5×10^{-4}
ω	$20\ \pi$ rad/hr

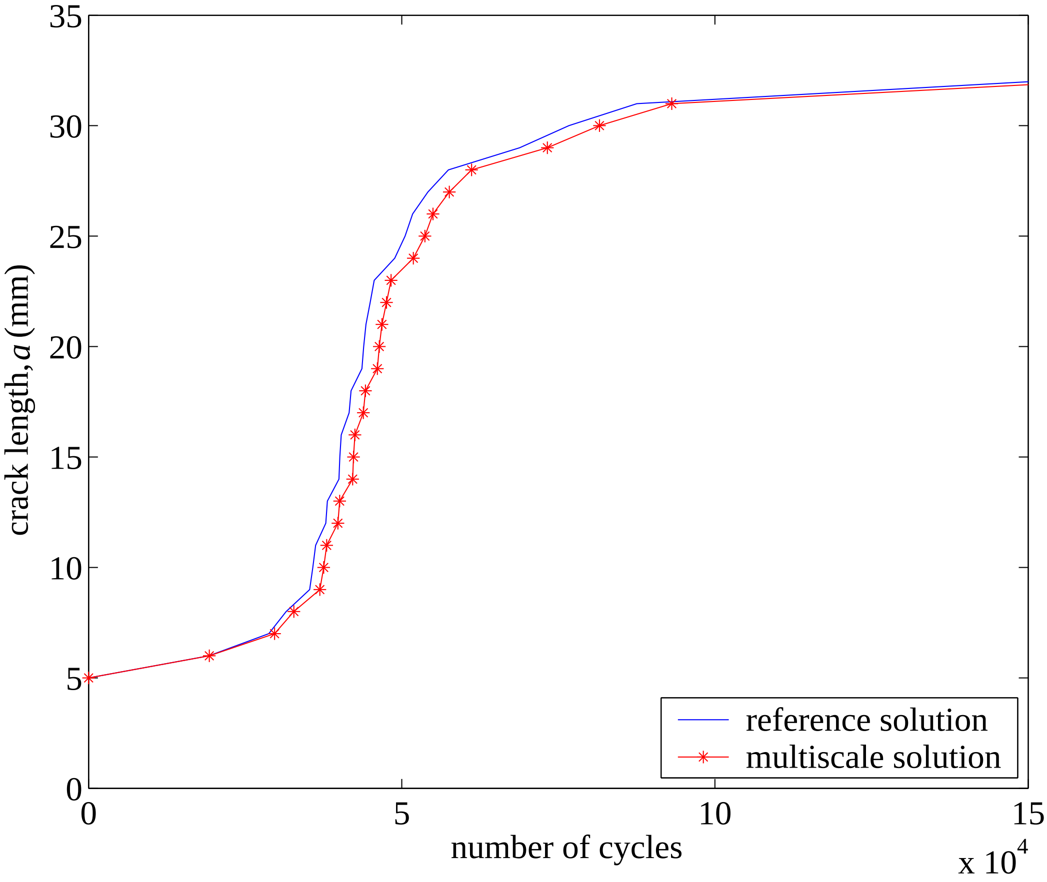

Figure 9: Fatigue life curve of the beam under periodic loading.

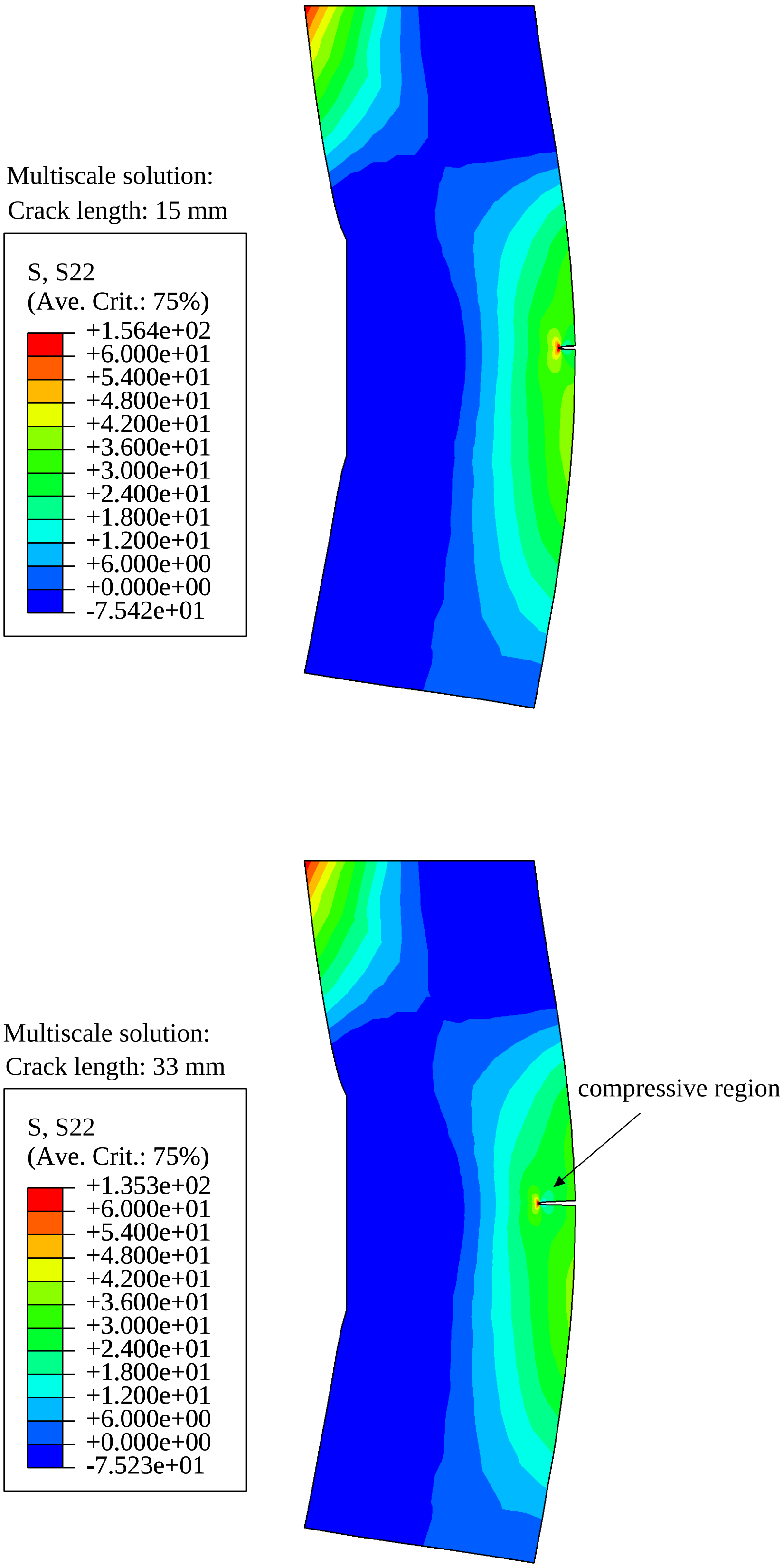

Figure 10: Stress distribution at the crack tip of the beam under periodic loading.

References

[1] P. C. Paris and F. Erdogan. A critical analysis of crack propagation laws. *J. Basic Engng.*, 85:528–534, 1963.

[2] M. H. El Haddad, T. H. Topper, and K. N. Smith. Prediction of non-propagating cracks. *Engng. Fracture Mech.*, 11:573–584, 1979.

[3] W. Elber. Fatigue crack closure under cyclic tension. *Engng. Fracture Mech.*, 2:37–45, 1970.

[4] R. G. Foreman, V. E. Keary, and R. M. Engle. Numerical analysis of crack propagation in cyclic-loaded structures. *J. Basic Engng.*, 89:459–464, 1967.

[5] M. Klesnil and P. Lukas. Influence of strength and stress history on growth and stabilisation of fatigue cracks. *Engng. Fracture Mech.*, 4:77–92, 1972.

[6] O. E. Wheeler. Spectrum loading and crack growth. *J. Basic Engng.*, 94:181–186, 1972.

[7] J. Fish. Hierarchical modeling of discontinuous fields. *Communications in Applied Numerical Methods*, 8:443–453, 1992.

[8] N. Sukumar, N. Moes, B. Moran, and T. Belytschko. Extended finite element method for three-dimensional crack modelling. *Int. J. Numer. Meth. Engng.*, 48(11):1549–1570, 2000.

[9] O. Nguyen, E. A. Repetto, M. Ortiz, and R. A. Radovitzky. A cohesive model of fatigue crack growth. *Int. J. Fracture*, 110(4):351–369, 2001.

[10] J. L. Chaboche. Continuum damage mechanics i: General concepts & ii: Damage growth, crack initiation and crack growth. *J. Appl. Mech.*, 55:59–72, 1988.

[11] C. L. Chow and Y. Wei. A model of continuum damage mechanics for fatigue failure. *Int. J. Fatigue*, 50:301–306, 1991.

[12] J. Fish and Q. Yu. Computational mechanics of fatigue and life predictions for composite materials and structures. *Comp. Meth. Appl. Mech. Engng.*, 191:4827–4849, 2002.

[13] A. Benssousan, J. L. Lions, and G. Papanicolaou. *Asymptotic Analysis for Periodic Structures*. North-Holland, Amsterdam, 1978.

[14] D. Krajcinovic and G. U. Fonseca. The continuous damage theory of brittle materials part 1: General theory. *J. Appl. Mech.*, 48:809–815, 1981.

[15] J. Najar. Continuous damage of brittle solids. In D. Krajcinovic and J. Lemaitre, editors, *Continuum Damage Mechanics: Theory and Applications*, pages 233–294. Springer-Verlag, Wien-New York, 1987.

[16] J. L. Chaboche. Continuous damage mechanics - a tool to describe phenomena before crack initiation. *Nucl. Engng. Design*, 64:233–247, 1981.

[17] J. C. Simo and J. W. Ju. Strain- and stress-based continuum damage models - i. formulation. *Int. J. Solids Structures*, 23(7):821–840, 1987.

[18] S. Suresh. *Fatigue of Materials*. Cambridge Univ. Press, Cambridge, UK, 1991.

[19] F. Erdogan. Crack-propagation theories. In H. Liebowitz, editor, *Fracture: An Advanced Treatise*, pages 497–590. Academic Press, 1968.

[20] X. P. Xu and A. Needleman. Numerical simulations of fast crack growth in brittle solids. *J. Mech. Phys. Solids*, 42(9):1397–1434, 1994.

[21] M. Ortiz and A. Pandolfi. Finite deformation irreversible cohesive elements for three dimensional crack-propagation analysis. *Int. J. Numer. Meth. Engng.*, 44:1267–1282, 1999.

[22] Q. Yu and J. Fish. Temporal homogenization of viscoelastic and viscoplastic solids subjected to locally periodic loading. *Computational Mechanics*, 29:199–211, 2002.

[23] J. Stoer and R. Bulirsch. *Introduction to Numerical Analysis*. Springer, New York, NY, 2nd edition, 1993.

[24] J. Pan, M. Saje, and A. Needleman. Localization of deformation in rate sensitive porous plastic solids. *Int. J. Fracture*, pages 261–278, 1983.

[25] J. Fish. *Finite Element Method for Localization Analysis*. Ph.d thesis, Northwestern Univ., Evanston, Il., 1989.

A Consistent tangent stiffness

In this appendix, the details of the derivation of (72) is presented. The macro-chronological damage evolution equation is expressed using (47). In case of a damage process (i.e., $\upsilon^{o} \geq \upsilon_{ini}$ and $\upsilon^{o}_{,\tau} > 0$), $\upsilon^{o}_{,\tau}$ may be defined as (exploiting the symmetry of $\hat{\mathbf{L}}$):

$$\upsilon^{o}_{,\tau} = \frac{1}{2\upsilon}\left(\mathbf{F}^{o}\hat{\boldsymbol{\varepsilon}}^{o}\right)\hat{\mathbf{L}}\left(\mathbf{F}^{o}\hat{\boldsymbol{\varepsilon}}^{o}\right)_{,\tau} \tag{88}$$

where,

$$\left(\mathbf{F}^{o}\hat{\boldsymbol{\varepsilon}}^{o}\right)_{,\tau} = (h^{o}_{\varsigma}\hat{\varepsilon}^{o}_{\varsigma})_{,\tau} = \left(\frac{\partial h^{o}_{\varsigma}}{\partial\hat{\varepsilon}^{o}_{\varsigma}}\hat{\varepsilon}^{o}_{\varsigma} + h_{\varsigma}\right)\frac{\partial\hat{\varepsilon}^{o}_{\varsigma}}{\partial\tau}; \quad \varsigma = 1,2,3 \tag{89}$$

in the cartesian coordinate system. Double indices do not imply summation convention in the above equation (and whenever Greek letters are used as indices). Differentiating (15) with respect to principal strain components:

$$\frac{\partial h^{o}_{\varsigma}}{\partial\hat{\varepsilon}^{o}_{\varsigma}} = \frac{a_1/\pi}{1 + a_1^2(\hat{\varepsilon}^{o}_{\varsigma} - a_2)^2} \tag{90}$$

The derivative of principal components of total strain tensor with respect to fast time coordinate, τ, may be computed using Hamilton's Theorem:

$$(\hat{\varepsilon}^{o}_{\varsigma})^3 - I_1(\hat{\varepsilon}^{o}_{\varsigma})^2 + I_2\hat{\varepsilon}^{o}_{\varsigma} - I_3 = 0 \tag{91}$$

where I_1, I_2 and I_3 are the invariants of the strain tensor:

$$I_1 = \mathrm{tr}(\boldsymbol{\varepsilon}^{o}) = \varepsilon^{o}_{ii} \tag{92a}$$

$$I_2 = \frac{1}{2}\left(\boldsymbol{\varepsilon}^{o} : \boldsymbol{\varepsilon}^{o} - I_1^2\right) = \frac{1}{2}\left(\varepsilon^{o}_{ij}\varepsilon^{o}_{ij} - \varepsilon^{o}_{ii}\varepsilon^{o}_{jj}\right) \tag{92b}$$

$$I_3 = \det(\boldsymbol{\varepsilon}^{o}) = \frac{1}{6}e_{ijk}e_{pqr}\varepsilon^{o}_{ip}\varepsilon^{o}_{jq}\varepsilon^{o}_{kr} \tag{92c}$$

in which $\mathrm{tr}(\cdot)$ and $\det(\cdot)$ denote trace and determinant of a second order tensor, respectively, and e_{ijk} is permutation symbol. Differentiating (91) with respect to τ yields to the following equation:

$$\frac{\partial\hat{\varepsilon}^{o}_{\varsigma}}{\partial\tau} = \frac{(\partial I_1/\partial\tau)(\hat{\varepsilon}^{o}_{\varsigma})^2 - (\partial I_2/\partial\tau)\hat{\varepsilon}^{o}_{\varsigma} + \partial I_3/\partial\tau}{3(\hat{\varepsilon}^{o}_{\varsigma})^2 - 2I_1\hat{\varepsilon}^{o}_{\varsigma} + I_2} \tag{93}$$

The fast time derivatives of the invariants may be obtained using (92):

$$\frac{\partial I_1}{\partial\tau} = \delta_{ki}\delta_{kj}\frac{\partial\varepsilon^{o}_{ij}}{\partial\tau} = E^{[1]}_{ij}\frac{\partial\varepsilon^{o}_{ij}}{\partial\tau} \tag{94a}$$

$$\frac{\partial I_2}{\partial\tau} = (\varepsilon^{o}_{mm}\delta^{o}_{ki}\delta^{o}_{kj} - \varepsilon^{o}_{ij})\frac{\partial\varepsilon^{o}_{ij}}{\partial\tau} = E^{[2]}_{ij}\frac{\partial\varepsilon^{o}_{ij}}{\partial\tau} \tag{94b}$$

$$\frac{\partial I_3}{\partial\tau} = \left(\varepsilon^{o}_{ik}\varepsilon^{o}_{kj} - \varepsilon^{o}_{kk}\varepsilon^{o}_{ij} - \frac{1}{2}\varepsilon^{o}_{mn}\varepsilon^{o}_{nm}\delta_{ik}\delta_{jk} + \frac{1}{2}\varepsilon^{o}_{mm}\varepsilon^{o}_{nn}\delta_{ik}\delta_{jk}\right)\frac{\partial\varepsilon^{o}_{ij}}{\partial\tau} = E^{[3]}_{ij}\frac{\partial\varepsilon^{o}_{ij}}{\partial\tau} \tag{94c}$$

Decomposing the total strain vector using (36b), exploiting the definition that macro-chronological strain tensor $\langle\boldsymbol{\varepsilon}^{o}\rangle$ to be independent of τ, $\partial\hat{\varepsilon}^{o}_{\varsigma}/\partial\tau$ in (94) may be replaced by $\partial\hat{\Psi}^{o}_{\varsigma}/\partial\tau$. Combining (89, 90, 93) and (94), we obtain:

$$\frac{\partial h^{o}_{\varsigma}\hat{\varepsilon}^{o}_{\varsigma}}{\partial\tau} = Z^{o}_{\varsigma ij}\frac{\partial\Psi^{o}_{ij}}{\partial\tau}; \qquad \varsigma = 1,2,3 \tag{95}$$

and,

$$Z^{o}_{\varsigma ij} = \left(\frac{a_1/\pi}{1+a_1^2(\hat{\varepsilon}^{o}_{\varsigma}-a_2)^2}\hat{\varepsilon}^{o}_{\varsigma}+h^{o}_{\varsigma} \right) \frac{E^{[1]}_{ij}(\hat{\varepsilon}^{o}_{\varsigma})^2 - E^{[2]}_{ij}\hat{\varepsilon}^{o}_{\varsigma}+E^{[3]}_{ij}}{3(\hat{\varepsilon}^{o}_{\varsigma})^2-2I_1\hat{\varepsilon}^{o}_{\varsigma}+I_2} \tag{96}$$

The fast time derivative of the damage equivalent strain, υ^{o}, may be expressed by combining (88, 95) and (96). In the vectorial form:

$$\upsilon^{o}_{,\tau} = \frac{1}{2\upsilon^{o}} \left(\mathbf{F}^{o}\hat{\boldsymbol{\varepsilon}}^{o}\right) \hat{\mathbf{L}}\mathbf{Z}^{o} : \boldsymbol{\Psi}^{o}_{,\tau} \tag{97}$$

where $\mathbf{Z}^{o}$ is a third order tensor given by (96). Finally, substituting the above equation into (47) yields:

$$\Lambda^{o}_{,\tau} = \mathbf{S} : \boldsymbol{\Psi}^{o}_{,\tau} \tag{98}$$

where,

$$\mathbf{S} = \left(\frac{\theta^{o}}{\omega^{o}}\right)^{\gamma} \frac{\partial\theta^{o}}{\partial\upsilon^{o}} \left[\frac{1}{2\upsilon^{o}} \left(\mathbf{F}^{o}\hat{\boldsymbol{\varepsilon}}^{o}\right) : \hat{\mathbf{L}}\mathbf{Z}^{o} \right] \tag{99}$$

The derivation of **R** is similar to the derivation of **S** and will not be presented separately. **R** may be obtained in the same way as **S** by replacing fast time variable, τ, by t, and evaluating the invariants of the strain tensor at $\tau = \tau_1$.

B Localization

In this appendix, the localization effect on the fatigue damage cumulative law is investigated. A simple bifurcation analysis outlined by Pan et al. [24] is employed. Given a homogeneously deformed body subjected to an incrementally applied static loading, an additional solution (alternative to the homogeneous one) is sought in which the incremental field quantities such as strain rate, $\dot{\boldsymbol{\varepsilon}}$ are discontinuous along a plane with a normal, $\mathbf{n}$. The general condition of bifurcation may be expressed as [25]:

$$(\mathbf{D} : \mathbf{n} \otimes \mathbf{n})\,\mathbf{m} = \mathbf{A}\mathbf{m} = 0 \tag{100}$$

where $\mathbf{D}$ is fourth order tangent stiffness tensor; $\mathbf{m}$ is a unit vector in the direction of the velocity field, and $\mathbf{A}(\mathbf{n})$ is a second order tensor. Localization occurs when the conditions of the above equation is met.

The constitutive equation of a material with continuous fatigue damage was given previously as (8b). Rewriting this equation in the rate form (omitting superscript ζ):

$$\dot{\boldsymbol{\sigma}} = (1-\omega)\mathbf{L} : \dot{\boldsymbol{\varepsilon}} - \dot{\omega}\mathbf{L} : \boldsymbol{\varepsilon} \tag{101}$$

In case of damage process, $\dot{\upsilon} \geq 0$ and $\upsilon > \upsilon_{ini}$, the damage law was expressed in rate form using:

$$\dot{\omega} = \left(\frac{\theta}{\omega}\right)^{\gamma} \frac{\partial\theta}{\partial\upsilon}\dot{\upsilon} \tag{102}$$

The damage equivalent strain υ is expressed using (12) or (13) and it is a function of the strain tensor only. Hence using the chain rule on (102), combining (101) and (102), and exploiting the symmetry of $\mathbf{L}$:

$$\dot{\boldsymbol{\sigma}} = \mathbf{D} : \dot{\boldsymbol{\varepsilon}} \tag{103}$$

where,

$$\mathbf{D} = \mathbf{L} : \left[(1-\omega)\mathbf{I} - \left(\frac{\theta}{\omega}\right)^{\gamma} \boldsymbol{\varepsilon} \otimes \frac{\partial\theta}{\partial\boldsymbol{\varepsilon}}\right] \tag{104}$$

B.1 Analysis of a one-dimensional fatigue model

A simplified analysis is conducted to evaluate the localization characteristics of the fatigue damage cumulative law. In a simple one-dimensional problem, the rate relation reduces to:

$$\dot{\sigma} = E\dot{\varepsilon} \left\{ \begin{array}{cc} (1-\omega) & \text{if} \quad |\varepsilon| < \varepsilon_{ini} \\ \left(1-\omega-\left(\frac{\phi}{\omega}\right)^{\gamma}\frac{\partial\theta}{\partial|\varepsilon|}|\varepsilon|\mathrm{H}(\dot{\varepsilon})\right) & \text{if} \quad |\varepsilon| \geq \varepsilon_{ini} \end{array} \right\} = E_t\dot{\varepsilon} \tag{105}$$

where $\dot{\sigma}$ and $\dot{\varepsilon}$ are stress and strain rates, respectively; ε is strain, E and E_t are elastic and tangent stiffnesses, respectively; $\varepsilon_{ini} = \upsilon_{ini}/\sqrt{(}.5E)$ is a threshold strain value, and $\mathrm{H}(\cdot)$ is the Heaviside step function operator. When the spring is subjected to monotonically increasing strain, the fatigue damage model reduces to a static damage law for a strain softening material. Hence, in this case, there exists a critical strain level, $\varepsilon_{cr}^{s} \geq \varepsilon_{ini}$ such that the tangent modulus is vanished:

$$E_t = \left(1 - \omega_{cr}^{s} - \left.\frac{\partial\theta}{\partial\varepsilon}\right|_{\varepsilon_{cr}^{s}} \varepsilon_{cr}^{s}\right) E = 0 \tag{106}$$

in which $\omega_{cr}^{s} = \omega(\varepsilon_{cr}^{s})$ is damage variable at the critical strain level. It is also worth mentioning that the ultimate strength of the material for monotonic loading is reached when $\varepsilon = \varepsilon_{cr}^{s}$.

For subcritical periodic loading with a constant strain amplitude, $\varepsilon_m^c < \varepsilon_{cr}^s$:

$$\frac{E_t}{E} \leq \psi \equiv 1 - \omega(N,\varepsilon) - \left(\frac{\phi}{\omega}\right)^{\gamma} \left.\frac{\partial\theta}{\partial\varepsilon}\right|_{\varepsilon_m^c} \varepsilon_m^c \tag{107}$$

where N is current number of load cycles. In this case, condition of localization reduces to $\psi = 0$ for positive elastic stiffness, E. Noting that $\omega \in [0,1)$ and $\phi/\omega \leq 1$, and considering $\gamma \equiv \gamma(N,\varepsilon)$ such that:

$$\gamma(N,\varepsilon) > \frac{\ln(1-\omega) - \ln(c_m)}{\ln(\theta) - \ln(\omega)}; \quad c_m = \left.\frac{\partial\theta}{\partial\varepsilon}\right|_{\varepsilon_m^c} \varepsilon_m^c \tag{108}$$

the fatigue damage cumulative law acts as a localization limiter, if $\phi < \omega$. In case, $\phi = \omega$, in addition to (108), θ in (105) is replaced by $\breve{\theta}$ such that:

$$\breve{\theta} = \min\left(tol\,\omega, \theta\right) \tag{109}$$

in which $tol \in (0,1)$.